Article published online: 2021-04-01

Synthesis and Solvatochromic Behavior of Zwitterionic Donor–Bridge–Acceptor Systems with Oligo(*p*-phenylene) Spacers

Irina Zharinova[a]
Nicolau Saker Neto[a]
Tze Cin Owyong[a]
Jonathan M. White[a]
Wallace W. H. Wong[*a]

[a] ARC Centre of Excellence in Exciton Science, School of Chemistry, Bio21 Institute, University of Melbourne, Parkville, Victoria 3010, Australia
wwhwong@unimelb.edu.au

Dedicated to Prof. Peter Bäuerle on his 65th birthday.

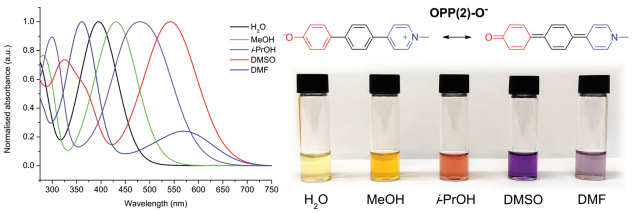

Received: 15.01.2021
Accepted after revision: 1.02.2021
DOI: 10.1055/s-0041-1725075; Art ID: om-21-0006oa

License terms:

© **2021**. The Author(s). This is an open access article published by Thieme under the terms of the Creative Commons Attribution-NonDerivative-NonCommercial License, permitting copying and reproduction so long as the original work is given appropriate credit. Contents may not be used for commercial purposes, or adapted, remixed, transformed or built upon. (https://creativecommons.org/licenses/by-nc-nd/4.0/)

Abstract Oligo(*p*-phenylene)s with a donor phenol group and an acceptor pyridinium moiety separated by one and two *p*-phenylene units were synthesized by the linear iterative Suzuki–Miyaura coupling method using aryl nonaflates as effective coupling reagents. Zwitterionic forms of these push–pull molecules were generated upon deprotonation of the phenol leading to large redshifts in absorbance maxima. UV-vis absorbance studies also revealed strong dependence of the band position on solvent polarity: a smooth bathochromic shift can be observed with the decrease of the solvent polarity. The molecule with one *p*-phenylene bridging unit showed the strongest solvatochromic characteristics in the series, spanning the range of 167 nm while moving from polar water to less polar *N*,*N*-dimethylformamide. The magnitude of this shift was close to Reichardt's dye — one of the most solvatochromic organic dyes known.

Key words conjugated molecules, cross-coupling, electron donor–acceptor systems, solvatochromism

Introduction

Push–pull organic molecules containing electron-rich and electron-poor moieties have seen application in sensors as well as optical and electronic devices.[1–4] They are discrete, functionally desymmetrized molecules, bearing electron donor and acceptor substituents as end-groups, separated by a π-conjugated bridge. Such organic systems can have large nonlinear optical (NLO) coefficients with ultra-fast responses originating from the almost instantaneous electronic polarization.[5–7] The π-conjugated bridges in these molecules are usually aromatic spacers, such as thienylene, phenylenevinylene, and phenylene units.[2,8,9]

One of the widely studied representatives of push–pull systems, Brooker's merocyanine (**BM**) (Figure 1), is composed of a strong donor phenolate group, an acceptor pyridinium group, and a vinyl linkage in between. It is known for its pronounced negative solvatochromic behavior [the hypsochromic shift of the absorbance maxima (λ_{max}) with the increase of the polarity of solvent] and its ease of preparation.[10,11] According to UV-vis spectroscopy measurements for **BM**, the absorbance maximum undergoes a large redshift while going from highly polar water (444 nm) to moderately polar pyridine (605 nm), a difference of 161 nm, accompanied by a color change from yellow to blue.[11] However, for sufficiently low polarity solvents (e.g. hydrocarbons), this solvatochromic behavior is reversed, and slight positive solvatochromism is observed instead.[12] Interaction between the oxygen atom of the merocyanine and the hydrogen atom of hydrogen bond donor solvents was found to be essential for the significant solvatochromic shift, as this bonding stabilized the zwitterionic form of the molecule.[13]

Another example displaying a negative solvatochromism moving from water (394 nm) to acetonitrile (472 nm) is 4-[*N*-methyl-4-pyridinio]-phenolate [**OPP(1)-O**$^-$, more commonly known as POMP], which is formed by directly attaching phenolate and pyridinium functionalities without any spacer (Figure 1).[14] One more well-known compound similar to **BM**

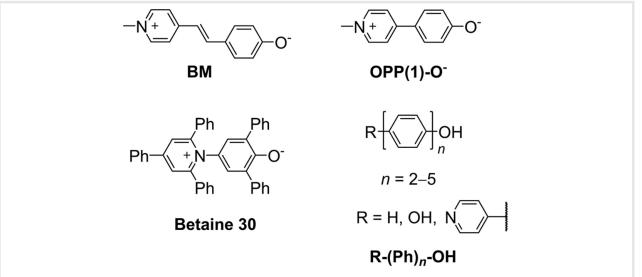

Figure 1 Some examples of organic molecules investigated for electro-optic applications.

and **OPP(1)-O**$^-$ is Reichardt's dye or **Betaine 30** (Figure 1).[3,15] This dye is extensively used as a probe for medium polarity. **Betaine 30** is constructed by directly connecting the nitrogen atom of the pyridyl moiety to the phenolate ring. A polarity scale has been established based on this compound, where the parameter $E_T(30)$ is defined as the molar electronic transition energy (kcal mol^{-1}) of Reichardt's betaine.[3] There is a linear correlation between the transition energies of **OPP(1)-O**$^-$ and **Betaine 30**; however, the former compound has smaller solvatochromic shifts than Reichardt's dye and is therefore less effective as a polarity indicator.[14]

The conjugation of push–pull chromophores can be extended by using oligo(*p*-phenylene)s (OPPs).[16,17] A series of OPPs with varying length and functionalized with one or two hydroxyl groups [**R-(Ph)$_n$-OH**] has been reported previously (Figure 1).[9] From UV-vis measurements for such systems, it was found that deprotonation leads to a bathochromic shift of the absorbance maximum by up to 80 nm in comparison to the protonated species. For the deprotonated forms of **R-(Ph)$_n$-OH** (R = H, OH; n = 3–5), there was a shift towards larger wavelengths as the donor number[18] of the solvent increased. The same behavior was also demonstrated in photoluminescence spectra. Therefore, by varying the solvent nature the emission wavelength of deprotonated OPPs can be tuned, which could be useful for the development of light-emitting materials.[19,20] This work was then extended by attaching an electron-accepting pyridyl moiety on the opposite end of an OPP chain terminated with an electron-donating hydroxyl group [**Py-(Ph)$_2$-OH**],[8] forming a donor–bridge–acceptor structure. In UV-vis spectra, the bathochromic shift of 118 nm was observed after treatment of a DMF solution with NaH.[8]

The described zwitterionic molecules could be represented in both aromatic and quinoid forms. The ground electronic state of these molecules was dominated by the charge-separated aromatic form, while the excited state was described by the neutral quinoid form with decreased resonance energy upon intramolecular charge transfer. The donor–bridge–acceptor topology and, especially, the donor/acceptor strength of substituents are crucial for varying the relative energetics of both resonance forms.[7]

To be useful for commercial devices, the priority in the synthesis of chromophores is given to cost-effective and high-yield chemical pathways. Of course, the synthetic approach for each class of NLO-chromophores could be different, but the molecules might involve similar fragments. A key to construct conjugated oligomers is to provide efficient carbon–carbon bond formation. Development of the field of organometallic catalysts using transition metal-catalyzed reactions has attracted attention for the synthesis of conjugated molecules. Among a large variety of transition metal catalysts, well-known examples are nickel- or palladium-based complexes.[21] In particular, Suzuki–Miyaura (SM) coupling[22] is an effective method for the synthesis of conjugated molecules with varying phenylene or other (hetero)aromatic units. Since its development, numerous improvements have been made with respect to reaction scope, application of various reaction substrates, lowering the catalyst loading, and ability to conduct reactions even at room temperature.[23,24]

For synthesis of conjugated chromophores such as OPPs, aryl/heteroaryl halides and triflates are generally used as substrates for SM coupling. Due to moderate reactivity of aryl triflates and their high cost, aryl nonaflates have been proposed as an improved alternative. Moreover, the main triflating reagent, triflic anhydride, is extremely reactive even at −78 °C, which can lead to side reactions. Nonafluorobutanesulfonyl fluoride ($C_4F_9SO_2F$, NfF), as the most convenient precursor for nonaflates, is a milder reagent. It is also nontoxic, air-stable, and can be stored for a long time,[25,26] whereas trifluoromethanesulfonyl fluoride is a poisonous gas. So far, only a few reports related to the application of aryl nonaflates in SM coupling have been published, where aryl/heteroaryl nonaflates have shown slightly higher reactivity and better yields compared to corresponding triflates.[27–29]

In this study, by extending the reported zwitterionic **OPP(1)-O**$^-$ system with one and two *p*-phenylene bridging units, we introduce new OPPs: **OPP(2)-O**$^-$ and **OPP(3)-O**$^-$ (Figure 2). The bridge selection was based on the structural simplicity and synthetic accessibility of OPPs and the similarity of the electron-poor pyridyl unit to the phenylene spacers of the chain. Additional substitutions were not sought to maintain as simple a system as possible and avoid confounding electronic effects. Figure 2 shows resonance structures of **OPP(*n*)-O**$^-$ (n = 1–3) where the zwitterionic structures are of aromatic character and the neutral forms have quinoid character. A reliable synthetic strategy involving SM coupling and nonaflate chemistry was implemented thus allowing sequential elongation of the chain to produce the desired OPPs. We also examine solvatochromic characteristics of new systems, compare them with the earlier studied analogue, and elucidate the chain-length effect on obtained properties.

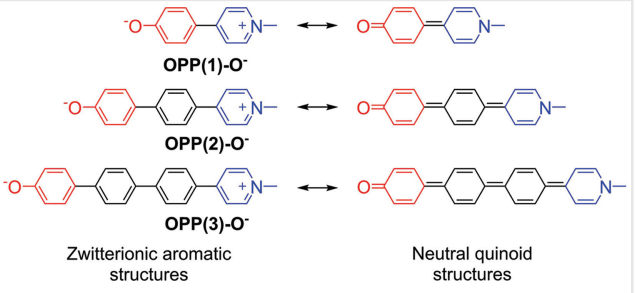

Figure 2 Resonance structures of **OPP(*n*)-O**$^-$ (n = 1–3).

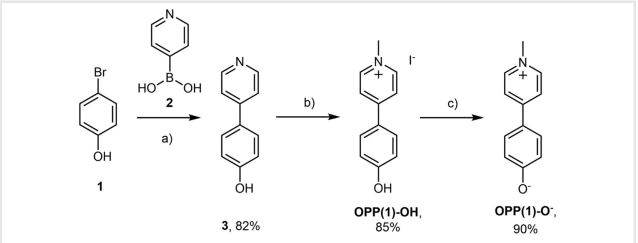

Scheme 1 Synthesis of *N*-methylpyridinium phenolate **OPP(1)-O**$^-$: a) Pd_2dba_3 (2.5 mol%), $Cy_3P{\cdot}HBF_4$ (6.0 mol%), K_3PO_4 (1.7 equiv), 1,4-dioxane/H_2O (2/1, v/v), 100 °C, 16 h; b) MeI (4.0 equiv), acetone, 55 °C, 16 h; c) NBu_4OH, MeOH, r.t., 15 min.

Results and Discussion

Synthesis

The previously reported molecule[14] **OPP(1)-O**$^-$ was synthesized in three consecutive steps (Scheme 1), starting from SM coupling of unprotected 4-bromophenol (**1**) and 4-pyridinylboronic acid (**2**). The initially applied SM reaction conditions were Pd_2dba_3 (0.5 mol%) and tBu$_3$P·HBF$_4$ (1.2 mol%) as a catalyst system, KF·2H_2O as a base, and THF at 60 °C,[30] but unsatisfactory conversion was observed, with a large amount of starting material remaining. After variation of reaction parameters including ligand (tBu$_3$P·HBF$_4$, Cy$_3$P·HBF$_4$, SPhos), base (KF, KF·2H_2O, K_3PO_4), solvent (THF, toluene, 1,4-dioxane, H_2O), and reaction temperature, the optimal combination was found to be Pd_2dba_3 (0.5 mol%), Cy$_3$P·HBF$_4$ (1.2 mol%), and K_3PO_4 in 1,4-dioxane/H_2O (2/1, v/v) at 100 °C,[31] which resulted in a yield of 82%. *N*-Methylation of **3** followed by deprotonation produced **OPP(1)-O**$^-$ in excellent yield (Scheme 1).

Linear iterative coupling with SM coupling chemistry was used as a method for extension of OPP bridges.[8,9,16] The starting 4-bromophenol (**1**) was benzylated to protect the phenol functionality that would ultimately be present in the final compound, and then coupled with 4-hydroxyphenylboronic acid (**5**) to form a simple biphenyl unit **6** in 70% yield (Scheme 2). In the first step of the cycle (Scheme 2), the phenol functionality of the substrate (**6** or **8**), unreactive in SM coupling, is activated by conversion to the nonaflate (**7** or **9**) using NfF.[25,27,29] Thus, in the second step the activated substrate couples with 4-hydroxyphenylboronic acid (**5**). As a result, one unit adds to the sequence at each cycle. The phenol group is recovered at the end of the cycle, and can then be activated in the next one.

N-Methylation reactions proceeded with high yields (98%) resulting in yellow precipitates of biphenyl and terphenylmethylpyridinium iodides (**12** and **13**) (Scheme 3). To further proceed, multiple debenzylation conditions were tested on **12,** such as TMS-I,[32] Pd/C hydrogenation,[33] $SOCl_2$,[34] and $NiCl_2{\cdot}6H_2O/NaBH_4$.[35] However, these showed only the presence of the unreacted starting material. Other trials[36] with LiI, LiCl, trifluoroacetic acid (TFA), formic acid, methanesulfonic acid, and molten pyridinium hydrochloride resulted in partial conversion to the product with a hydroxyl group, as determined by ESI-MS. To ensure full debenzylation of **12** and **13,** rather harsh conditions were applied, with stirring in excess HBr/AcOH (33 wt%) at room temperature.[37] ESI-MS confirmed conversion of the benzyl ether to an acetate group, as well as small amounts of the protonated final products **OPP(2)-OH**

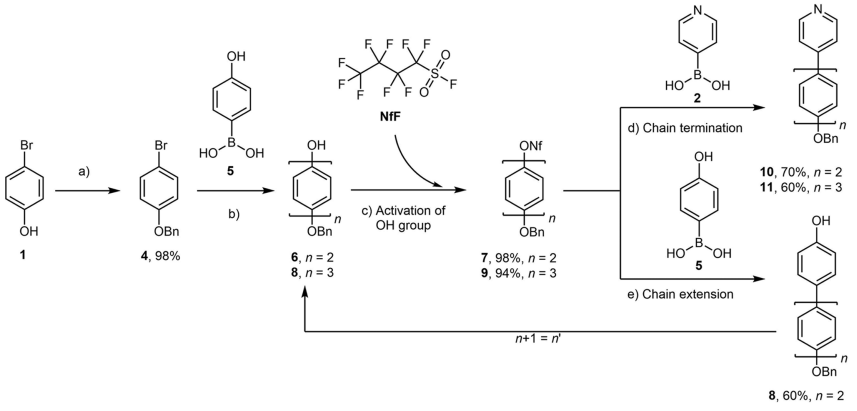

Scheme 2 Synthesis of OPPs via linear iterative coupling: a) BnCl (1.1 equiv), K_2CO_3 (3.0 equiv), KI (10 mol%), acetone, 60 °C, 5 h; b) Pd_2dba_3 (0.5 mol %), Cy$_3$P·HBF$_4$ (1.2 mol%), K_3PO_4 (1.5 equiv), 1,4-dioxane/H_2O (2/1, v/v), 100 °C, 16 h; c) NfF (1.2 equiv), Et_3N (1.5 equiv), DCM, r.t. for $n = 2$ or DMF, 60 °C, 16 h for $n = 3$; d) $n = 2$: Pd_2dba_3 (0.5 mol%), Cy$_3$P·HBF$_4$ (1.2 mol%), K_3PO_4 (1.7 equiv), 1,4-dioxane/H_2O (2/1, v/v), 100 °C, 16 h; $n = 3$: Pd_2dba_3 (2.5 mol%), Cy$_3$P·HBF$_4$ (6.0 mol%), K_3PO_4 (1.7 equiv), THF/H_2O (10/1, v/v), 100 °C, 16 h; e) Pd_2dba_3 (0.5 mol%), Cy$_3$P·HBF$_4$ (1.2 mol%), K_3PO_4 (1.7 equiv), 1,4-dioxane/H_2O (2/1, v/v), 100 °C, 16 h.

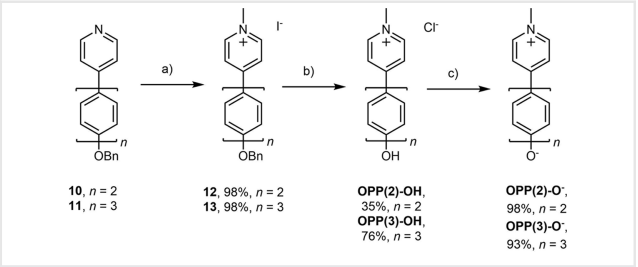

Scheme 3 *N*-Methylation and deprotection of extended OPPs: a) MeI [5.5 equiv ($n = 2$) or 4.4 equiv ($n = 3$)], DMF, 60 °C, 48 h; b) HBr/AcOH (excess), r.t., 16 h; HCl (excess), MeOH, reflux; c) Aqueous NaOH, r.t.

and **OPP(3)-OH**, with no detectable trace of remaining benzylated material.

In the case of biphenylmethylpyridinium iodide **12**, the obtained mixture of the acetate (**14**) and **OPP(2)-OH** was subjected to base deprotection (Scheme 4). ^{1}H NMR spectroscopy revealed the presence of the main deprotonated molecule **OPP(2)-O$^-$** as well as a byproduct with similar structure. Analysis of the byproduct signals in the ^{1}H NMR spectrum showed that its most shielded doublet had half the integration of all other byproduct aryl signals, suggesting substitution of the hydrogen atom *ortho* to the phenolate, and ^{13}C NMR spectroscopy displayed an unexpectedly shielded signal at 93 ppm, consistent with an aryl iodide (iodobenzene ^{13}C–I signal = 95 ppm). ESI-MS confirmed the presence of *o*-iodo-substituted teraryl (**15**) as a side product, matching the theoretical mass ($[M + H]^+$ $m/z = 388.0193$).

One of the explanations for the *o*-iodination observed is that the solution of HBr/AcOH used could degrade slowly producing some amount of Br_2, evidenced by the light orange color of the acid mixture. During the debenzylation of the *N*-methylpyridinium iodide salt, Br_2 could partially oxidize the iodide to molecular I_2 and the triiodide anion I_3^-.

The subsequent basic deprotection conditions lead to the formation of phenolates, which are highly electron-rich and thus allowed electrophilic *o*-iodination to occur.

To avoid the undesirable electrophilic iodination, the workup procedure was modified in order to remove any iodine/triiodide traces. The solids obtained after the HBr/AcOH reaction were washed with a sodium metabisulfite solution as a reducing agent. An acidic deacetylation pathway

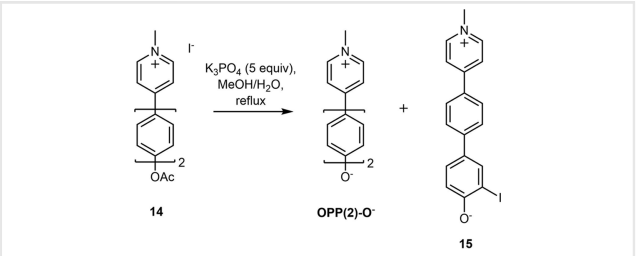

Scheme 4 Deacetylation procedure using K_3PO_4.

was used and followed by a deprotonation step. To ensure a uniform counterion for all species, the obtained deprotonated forms were treated with aqueous HCl to produce the chloride salts **OPP(2)-OH** and **OPP(3)-OH** with 35% and 76% yields, and the compounds were stored in this form for prolonged periods. When desired, the substances were subjected to a final deprotonation with aqueous NaOH, with almost quantitative conversion to **OPP(2)-O$^-$** and **OPP(3)-O$^-$** (Scheme 3).

All obtained intermediates and final products were characterized by ^{1}H NMR [except **OPP(3)-O$^-$** due to the low solubility] and ^{13}C NMR [except **11**, **OPP(2)-O$^-$**, and **OPP(3)-O$^-$** due to the low solubility] spectroscopy, mass spectrometry, and FT-IR.

Structural Characterization

^{1}H NMR spectroscopy in DMSO-d_6 (collected at 25 °C, ~10 mmol/L) confirmed the presence of the phenol functionalities of **OPP(*n*)-OH** ($n = 1$–3). Upon treatment with the base, the solubility of the deprotonated forms **OPP(*n*)-O$^-$** ($n = 1$–3) drops dramatically making NMR characterization difficult [see the Supporting Information (SI)].

The ^{1}H NMR spectrum of **OPP(2)-OH** showing a set of six doublets integrating to two and the most deshielded singlet integrating as one corresponds to the phenol hydroxyl. The ^{1}H NMR spectrum of **OPP(2)-O$^-$** (collected at 60 °C) shows a 0.4 ppm shift for the most shielded doublet upon deprotonation and disappearance of the OH signal (Figure 3).

The crystal structures of **OPP(1)-OH** and **OPP(1)-O$^-$** have been reported previously.[38] In this work, single crystals of the elongated oligomers were obtained by slow diffusion of diethyl ether vapor into a solution of sodium methoxide in methanol or DMSO solution of compounds **OPP(2)-OH** and **OPP(3)-OH**. ORTEP representations of the obtained crystal structures are depicted in Figure 4 and derived parameters are given in Table S1 (SI).[39] Comparison of the crystal structure for **[OPP(2)-O$^-$]$_2$·HCl** was complicated by the fact that the unit cell contained two equivalent molecules sharing one hydrogen atom as well as one chloride counterion. Thus, the diffraction parameters obtained referred neither to the fully deprotonated **OPP(2)-O$^-$** nor the fully protonated **OPP(2)-OH** molecules, but rather an in-between state. The structure of **OPP(3)-OH** is fully protonated and has a chloride counterion. The C–O bond lengths for the obtained teraryl and quateraryl compounds [1.335(2) Å and 1.364(3) Å] are closer to that of **OPP(1)-OH** [1.363(6) Å] indicating rather aromatic character of the structures, whereas the C–O bond length of 1.305(2) Å in **OPP(1)-O$^-$** is shorter. The dihedral angles between the pyridinium moieties and their adjacent rings for **[OPP(2)-O$^-$]$_2$·HCl** and **OPP(3)-OH** are similar (15.8° and 15.0°). Meanwhile, this value is lower for **OPP(1)-O$^-$** (5.7°),

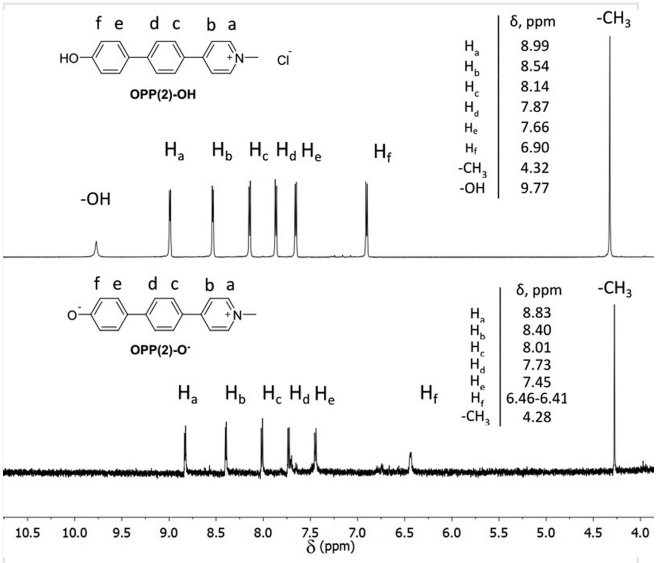

Figure 3 Comparison of ^{1}H NMR in DMSO-d_6 for **OPP(2)-OH** and **OPP(2)-O$^-$** (collected at 25 °C and 60 °C, ~10 mmol/L).

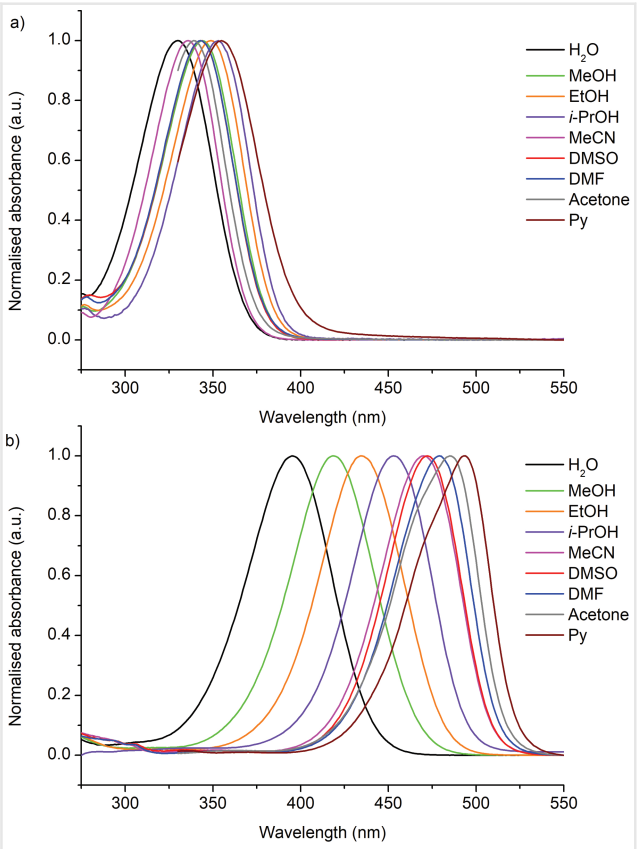

Figure 5 UV-vis absorbance spectra of **OPP(1)-OH** (a) and **OPP(1)-O$^-$** (b) in solvents of different polarity.

reflecting the enhanced quinoid character of the structure. The positive bond-length alternation value calculated with crystal-structure data for **OPP(1)-O$^-$** suggests a predominantly quinoid-type structure.[38] In contrast, the small negative value calculated for **[OPP(2)-O$^-$]$_2$·HCl** points to moderately zwitterionic character (Table S1, SI), likely due to the partial protonation.

UV-vis Absorbance Spectroscopy

UV-vis data were collected for the **OPP(*n*)-OH** and **OPP(*n*)-O$^-$** ($n = 1$–3) series in a range of solvents of different polarity (Figures 5-8). The solvent polarity scale was adopted from Reichardt's work.[3] Absorbance maxima are provided in Table 1, as well as comparison with literature values[14] for **OPP(1)-O$^-$**. Solvent choice was limited by solubility of the compounds, with lower polarity solvents such as chloroform or petroleum spirits not forming stable solutions of sufficient concentration. As was reported previously,[9] deprotonated species exist in protic solvents only for a short time, and undergo fast protonation. For this reason, these solutions should be prepared directly before the measurements, and stabilized with an excess of base (>20 equiv).

Absorbance profiles for the protonated compounds **OPP(*n*)-OH** ($n = 1, 2$) showed one band, whose position did not uniformly shift in correlation with the solvent polarity (Figures 5a and 6a; Table 1). Upon deprotonation, a

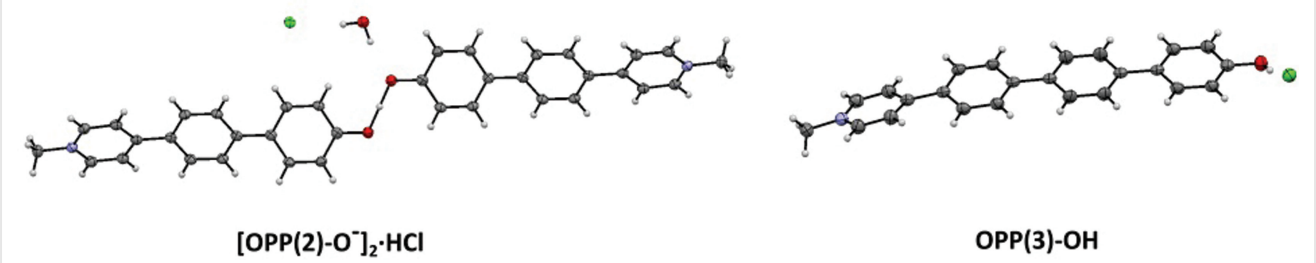

Figure 4 Crystal structures of **[OPP(2)-O$^-$]$_2$·HCl** and **OPP(3)-OH**.37 Thermal ellipsoids are drawn at the 50% probability level.

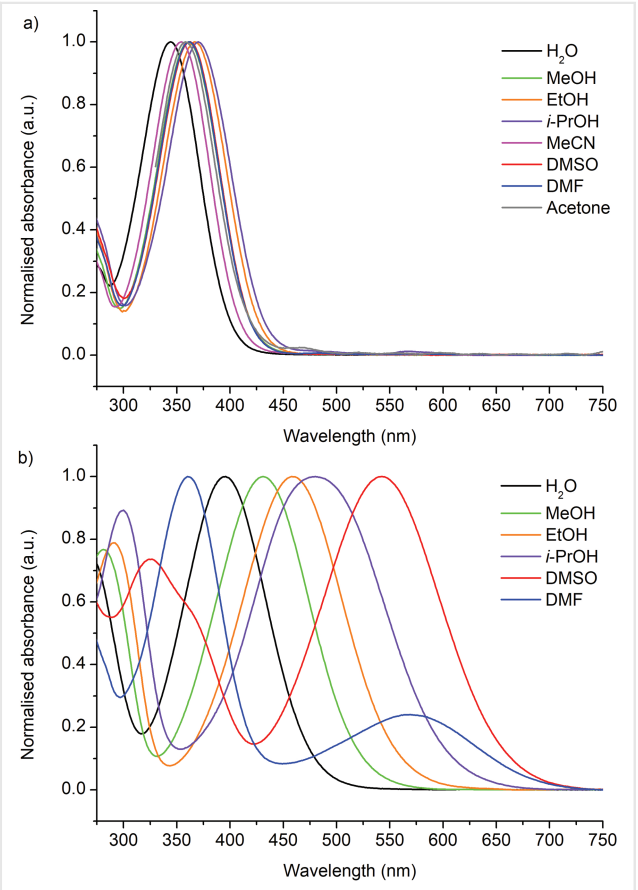

Figure 6 UV-vis absorbance spectra of **OPP(2)-OH** (a) and **OPP(2)-O**$^-$ (b) in solvents of different polarity.

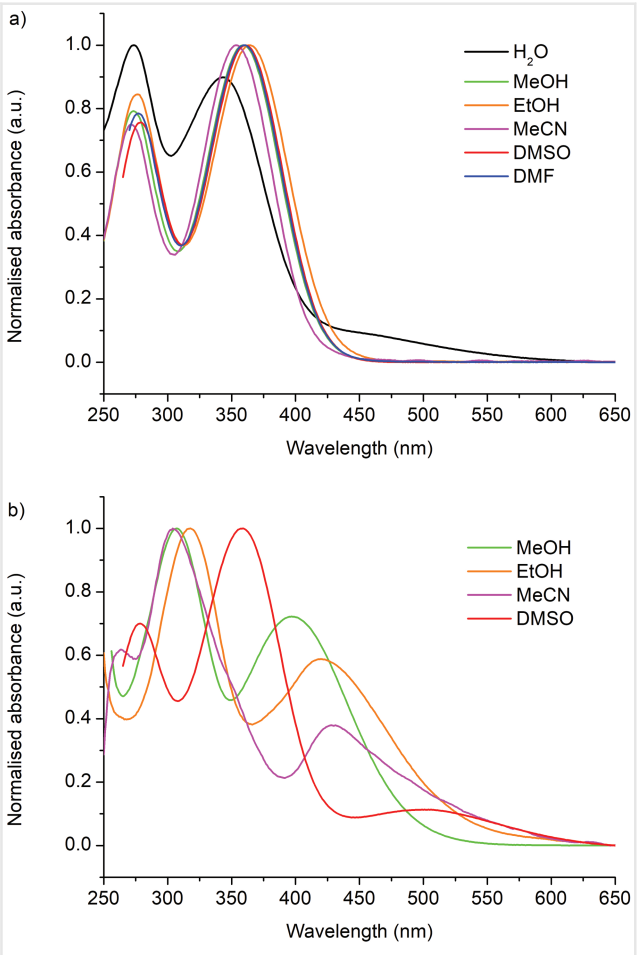

Figure 8 Absorbance spectra for **OPP(3)-OH** (a) and **OPP(3)-O**$^-$ (b) in solvents of different polarity.

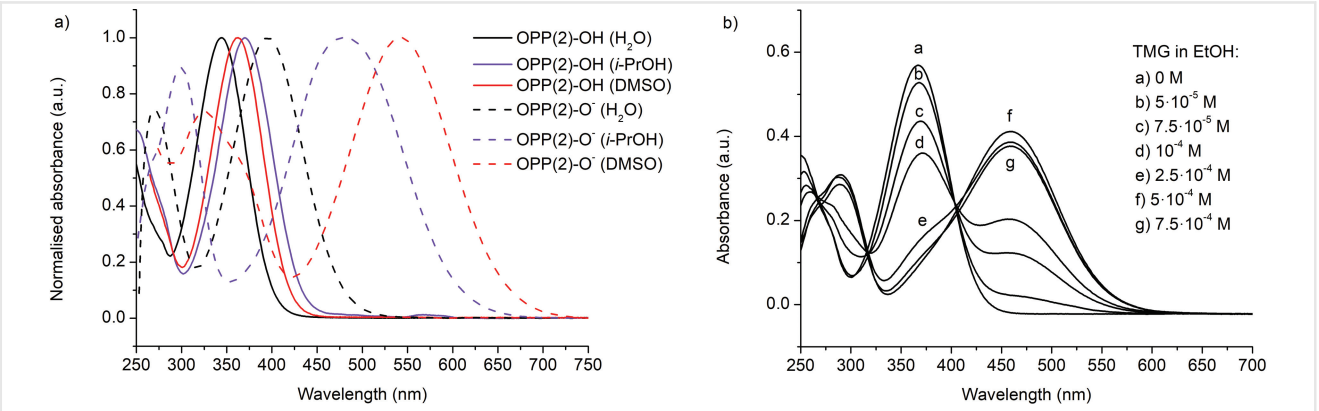

Figure 7 UV-vis absorbance spectra: a) comparison of **OPP(2)-OH** (solid lines) and **OPP(2)-O**$^-$ (dashed lines) in H_2O, *i*-PrOH, and DMSO; b) **OPP(2)-OH** (3×10^{-5} M) in EtOH in the presence of various amounts of TMG.

bathochromic shift was observed in all solvents and there was a drastic effect of the medium polarity on position of the absorbance spectra of **OPP(*n*)-O**$^-$ ($n = 1, 2$) (Figures 5b and 6b; Table 1). In the case of **OPP(1)-OH**, solutions in EtOH, DMF, and pyridine were stabilized with TFA (~10 equiv) as the solutions prepared in pure solvent showed

Table 1 Absorbance maxima obtained for **OPP(*n*)-OH** and **OPP(*n*)-O$^-$** in solvents of different polarity

E_T(30), kcal mol^{-13}	λ_{max} abs, nm						
	Solvent	**OPP(1)-OH**	**OPP(1)-O$^-$** (ref. 13)	**OPP(2)-OH**	**OPP(2)-O$^-$**	**OPP(3)-OH**	**OPP(3)-O$^-$**
40.5	Pyridine	355	494 (–)	*	*	*	*
42.2	Acetone	339	485 (479)	358	*	*	*
43.2	DMF	343	479 (–)	362	360, 563	277, 360	*
45.1	DMSO	343	472 (473)	363	326, 543	279, 361	279, 359, 504
45.6	MeCN	336	470 (472)	354	*	271, 354	263, 304, 431
48.4	*i*-PrOH	353	453 (457)	370	300, 480	*	*
51.9	EtOH	349	434 (–)	367	290, 458	277, 365	318, 420
55.4	MeOH	344	419 (418)	361	281, 431	273, 359	307, 397
63.1	H_2O	330	395 (394)	344	396	274, 343	*

*Values not obtained due to low solubility.

the presence of the deprotonated form (Figure S1, SI). Comparing the shifts between **OPP(1)-OH** and **OPP(1)-O$^-$**, there is a 64 nm difference in the highest polarity solvent (water), while in moderately polar acetonitrile the difference grows to 128 nm, reaching the largest bathochromic shift of 139 nm in the least polar solvent studied, pyridine.

The simplest zwitterionic compound obtained in this work, the *N*-methylpyridinium phenolate, **OPP(1)-O$^-$**, was thoroughly studied in order to reproduce the spectroscopic characteristics reported by Diemer et al.[14] (Figure 5b). It was mentioned that the basicity of the analyzed solution played an important role in obtaining reliable data, though the nature of the base used was not specified. Thus, several bases were explored — NaOH (added as an aqueous solution), NaH, *t*-BuOK, and 1,1,3,3-tetramethylguanidine (TMG). Spectra acquired with the addition of the aqueous solution of NaOH were 15–20 nm blueshifted compared with the literature values.[14] It was possible that the addition of even small amounts of water considerably affected the solvation shell of the molecules in organic solvents. Usage of NaH and *t*-BuOK could not provide a full set of data, as these strong bases reacted with some solvents. Ultimately, we opted for the use of TMG[40] for stabilization of all **OPP(*n*)-O$^-$** species in the measured solutions, as it is a strong base which is fully miscible with water and most organic solvents. The maximum absorbance wavelengths derived for **OPP(1)-O$^-$** solutions with the addition of TMG are in good agreement with the reported values[14]: 419 and 418 nm in MeOH, 470 and 472 nm in MeCN, and 485 and 479 nm in acetone (Table 1).

Focusing on the absorbance spectra of **OPP(1)-O$^-$** in different solvents, a smooth bathochromic shift was observed with the decrease of the solvent polarity. The maximum absorbance wavelength changed from 395 nm for water to 494 nm for pyridine (Figure 5b, Table 1), thus demonstrating almost a 100 nm shift towards longer wavelengths and negative solvatochromic behavior.

UV-vis spectra for **OPP(2)-OH** and **OPP(2)-O$^-$** are shown in Figure 6a and Figure 6b). Deprotonation induces a spectral shift towards longer wavelengths with a change of 52 nm for water, 110 nm for *i*-PrOH, and a particularly pronounced value of 180 nm for DMSO (Figure 7a). Study of **OPP(2)-O$^-$** behavior in solution reveals strong negative solvatochromism as the lowest energy transition is redshifted by 167 nm moving from highly polar water to comparatively lower polarity DMF (Figure 6b). This shift is almost twice that measured for **OPP(1)-O$^-$** (84 nm). Also, in contrast to **OPP(1)-O$^-$**, the absorbance profiles of **OPP(2)-O$^-$** show at least two distinct maxima. Uniquely, in DMF solution, the most redshifted absorbance feature was no longer the most intense transition.

An additional study was carried out to track spectral changes between **OPP(2)-OH** and **OPP(2)-O$^-$**. UV-vis spectra were acquired for the ethanol solutions of the protonated form **OPP(2)-OH** with a varying concentration of TMG (Figure 7b). The band at 367 nm gradually decreased and then disappeared completely while new bands at 290 and 458 nm arose upon increasing the TMG content in the solution, with isosbestic points visible around 316 and 406 nm. This observation confirms that the former band at 367 nm originates from the protonated species **OPP(2)-OH** and the latter redshifted one at 458 nm from the deprotonated ones of **OPP(2)-O$^-$**.

The absorbance spectra of **OPP(3)-OH** and **OPP(3)-O$^-$**, containing two phenylene spacers, are shown in Figure 8a and Figure 8b, and the band positions are summarized in Table 1. The effect of solvents on the photophysical properties of these species was quite different from the shorter molecules. The absorbance profile for **OPP(3)-OH** composed of two absorbance maxima, indicating two possible transitions in the measured wavelength range. Upon deprotonation, changes in spectral shapes and band

positions were not consistent with polarity medium variations. One possible explanation is that the increased number of slightly twisted phenylene spacers hinders electron delocalization between the donor and acceptor ends, nearing the effective conjugation length for the system in solution. Interestingly, in most cases, the absorbance maximum for **OPP(3)-O**$^-$ in the visible region was situated at shorter wavelengths than for **OPP(2)-O**$^-$ (in MeOH 397 nm vs. 432 nm). It has been previously observed that the redshift in extended donor–acceptor OPPs is often saturated for biphenyl or terphenyl chains.[41] Furthermore, the low solubility of the extended OPPs meant that aggregation effects could become important. Rod-like zwitterionic compounds are prone to forming *head–tail* dimers even in dilute solution.[42] This could suppress solvatochromic variations, especially in lower polarity solvents which would have difficulty breaking apart the ionic pairs. However, dilution experiments (Figure S5, SI) suggested that this was not a major factor for **OPP(3)-O**$^-$ in DMSO.

Electronic transition energies (E_T, kcal mol^{-1}) were estimated for **OPP(*n*)-O**$^-$ using the most redshifted absorbance maxima ($E_T = 28591/\lambda_{max}$).[3] Figure 9 shows the dependence of the transition energies on the polarity of the solvent for **OPP(*n*)-O**$^-$ and **Betaine 30**. Data points were interpolated with the best linear fit, and the fitting parameters derived (Table S8, SI). Thus, among the studied examples, the slope for **OPP(2)-O**$^-$ (1.09 ± 0.10) is equal to that for **Betaine 30** (unity, by definition) within the error margin, suggesting that the dyes are comparably solvatochromic within the explored polarity range. This is noteworthy, as **Betaine 30** is among the most solvatochromic organic dyes known.[13] Like **Betaine 30**, **OPP(2)-O**$^-$ can be used as a polarity indicator.

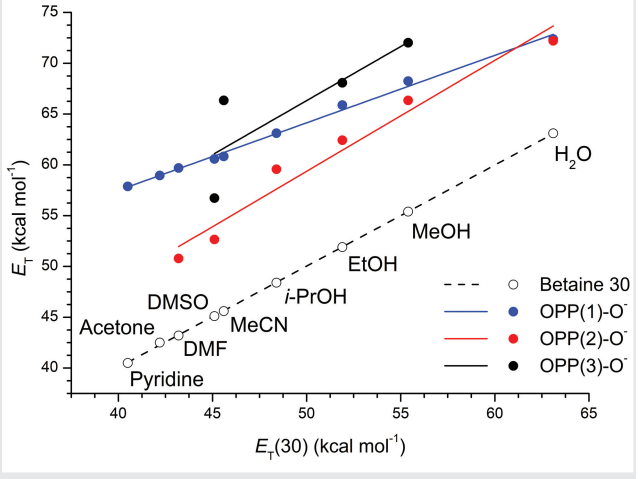

Figure 9 Transition energies of **Betaine 30** and **OPP(*n*)-O**$^-$ versus the empirical parameter of polarity E_T(30).

The negative solvatochromic behavior of **OPP(2)-O**$^-$ may be diminished in low polarity solvents (hydrocarbons, chlorinated solvents, etc.) as the system approaches a possible solvatochromic reversal region (similar to **BM**).[12] However, due to solubility limitations for **OPP(2)-O**$^-$, this cannot be easily verified.

Theoretical Studies

Several theoretical studies have been reported for **OPP(1)-O**$^-$ as a model compound.[43–45] However, the comparison of calculated structural and spectroscopic characteristics with experimental data is complicated by their strongly solvent-dependent nature. Therefore, solvation effects should be taken into consideration when performing molecular simulations.[46,47] The negative solvatochromic behavior of **OPP(1)-O**$^-$ has been comprehensively investigated with calculations in solvents of different polarity by implementing various solvation models using density functional theory (DFT) and time-dependent DFT (TD-DFT) methods,[48] showing qualitative agreement with experimental results. Based on these findings, we carried out calculations for **OPP(*n*)-O**$^-$ (n = 1–3). Using the GAUSSIAN16 software suite,[49] the ground-state geometry was optimized using the M06-2X functional and 6-31 + G (d,p) basis set, while TD-DFT calculations were performed at the CAM-B3LYP/6-31 + G** level of theory. To complement the calculations performed under vacuum, implicit solvation was performed using a polarizable continuum model for H_2O (ε = 78.39), DMSO (ε = 46.70), and acetone (ε = 20.70) included in both geometry optimization and energy calculations. The results obtained are given in Table S10 (SI). Figure 10a shows optimized geometries and frontier molecular orbitals of **OPP(*n*)-O**$^-$ (n = 1–3) under vacuum. It should be noted that the structures were planar and HOMOs and LUMOs were delocalized throughout the chain even upon moving to extended analogues.

Meanwhile, calculations with implicit solvation resulted in geometric and electronic differences. The optimized geometries of **OPP(2)-O**$^-$ and **OPP(3)-O**$^-$ were no longer fully planar, with a small amount of twisting present between the rings. Figure 10b compares the HOMOs and LUMOs for OPPs in vacuum and aqueous medium. In the case of **OPP(1)-O**$^-$, the HOMO and LUMO distribution in water stayed the same as in the vacuum, while the energy levels were slightly lowered.

Considering **OPP(2)-O**$^-$, it was clearly seen that solvation triggered a spatial separation of the orbitals; as expected, the HOMO concentrated around the donor phenolate group while the LUMO moved towards the acceptor pyridinium unit, with small amounts of both orbitals still overlapping on the phenylene spacer. The trend

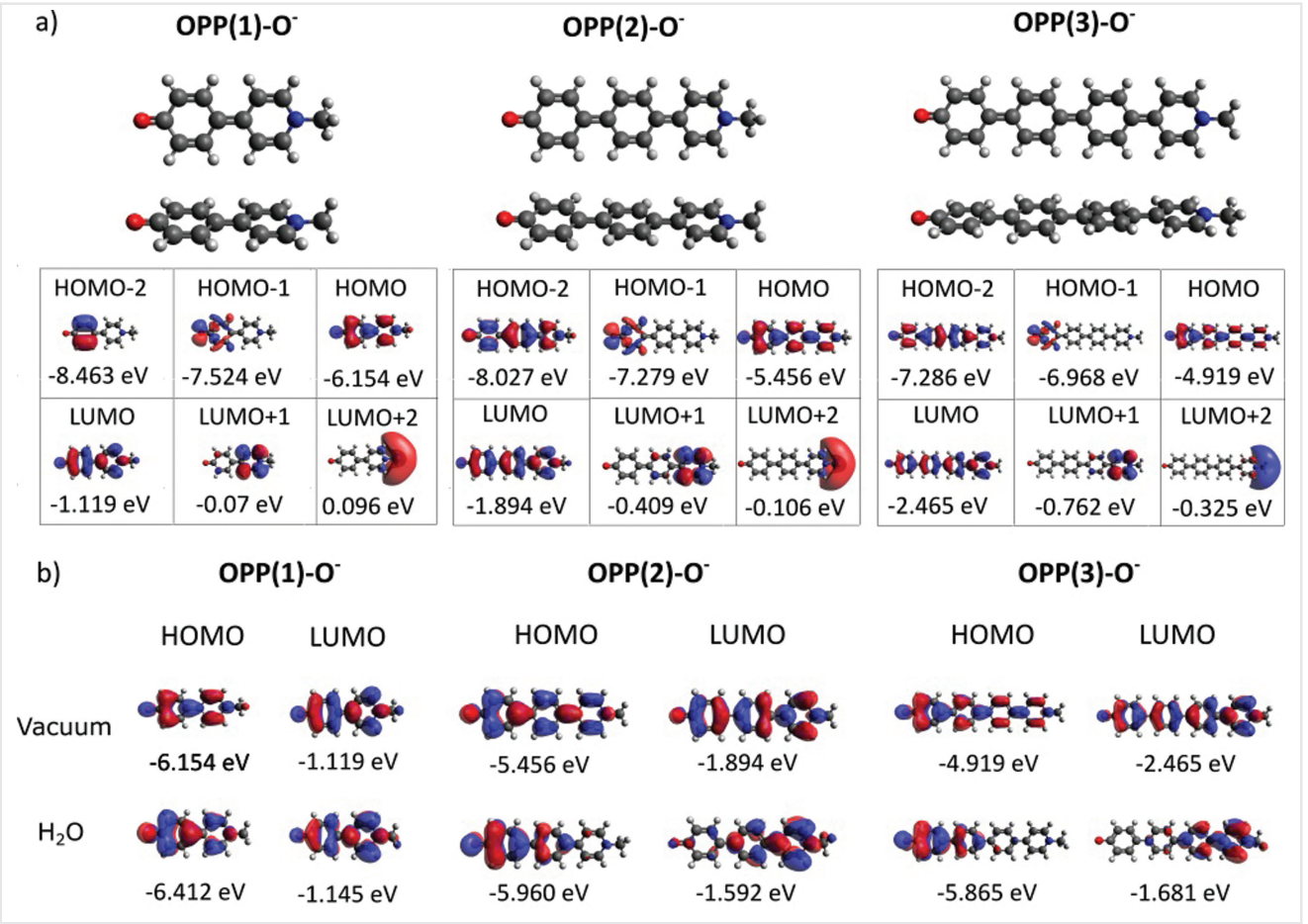

Figure 10 a) Optimized geometries and frontier molecular orbitals of **OPP(*n*)-O**$^-$ (n = 1–3) in vacuum, b) HOMO and LUMO of **OPP(*n*)-O**$^-$ (n = 1–3) in vacuum and H_2O.

towards separation of the orbitals continued for the quateraryl structure **OPP(3)-O**$^-$, where now the HOMO and LUMO no longer overlapped on the π-conjugated bridge. These calculations suggest that even modestly sized *p*-phenylene bridges can greatly hinder electron delocalization between the donor and acceptor ends in zwitterionic OPPs. In general, for **OPP(2)-O**$^-$ and **OPP(3)-O**$^-$ in H_2O, DMSO, or acetone, HOMO energies were lowered, while LUMO energies were raised compared with the values in vacuum. It is also worth noting the sharp increase of the ground-state dipole moments upon implicit solvation, in all cases roughly doubling relative to the vacuum calculations (Table S10, SI).

Conclusions

Zwitterionic OPPs with a donor phenolate group and an acceptor pyridinium moiety separated by one and two *p*-phenylene units were synthesized by the linear iterative coupling method using aryl nonaflates as effective coupling reagents, thus producing teraryl and quateraryl systems with good yields. For the studied **OPP(*n*)-OH** and **OPP(*n*)-O**$^-$ systems (n = 1–3), a bathochromic shift occurred in absorbance spectra upon deprotonation. Also for deprotonated species, a redshift of the absorbance maxima was observed with decreased solvent polarity. The introduction of a *p*-phenylene spacer between the phenolate and pyridinium moieties in **OPP(2)-O**$^-$ caused the molecule to display more extreme solvatochromic behavior when compared to **OPP(1)-O**$^-$, increasing the solvatochromic shift from 84 to 167 nm while moving from water to DMF.

The magnitude of this shift is close to the strongly solvatochromic **Betaine 30**. In contrast, for the elongated system **OPP(3)-O**$^-$, the absorbance spectrum blueshifted compared to the shorter molecules.

Based on the data obtained, further extension of the chain ($n \geq 4$) is unlikely to produce compounds with more redshifted absorbance in solution, as the HOMO and LUMO are expected to become more localized at the ends of the molecule, increasing their energetic separation. This can be taken as a measure of the degree of electron

delocalization permitted through *p*-phenylene bridges. A fuller experimental investigation of longer zwitterions would require the preparation of *p*-phenylene spacers containing solubilizing groups, such as alkyl substituents. However, these modifications must be performed in such a way to avoid excessive electronic influences on the molecule, and to not induce further dihedral twisting of the *p*-phenylene rings.

Experimental Section

Commercial reagents were purchased from Sigma-Aldrich, AK Scientific, Matrix Scientific, Boron Molecular, Ajax Finechem, Univar, and Labchem, and were used as delivered. Commercially available NfF was stirred with K_2HPO_4/K_3PO_4 (1:1, pH = 12–13) concentrated aqueous buffer for 96 h, filtered, and distilled over P_2O_5 to remove perfluorosulfolane.[50] Anhydrous dichloromethane was obtained from alumina-packed drying columns,[51] and anhydrous DMF and Et_3N were obtained by drying over activated molecular sieves. Standard Schlenk techniques were used for air-sensitive reactions. For oxygen-sensitive reactions, solvents were sparged with nitrogen gas for 30 min prior to addition, and the systems were closed with a rubber septum and maintained under positive nitrogen pressure. Purification via flash column chromatography was performed with Merck-Millipore silica gel (Kieselgel 60, 40–63 µm, 230–400 mesh). Thin-layer chromatography was performed on Merck-Millipore Silica gel 60G F_{254} glass plates, and spots were revealed under 254 and 365 nm light from a mercury lamp.

^{1}H NMR (400, 500, and 600 MHz) and ^{13}C NMR (101, 126, 151 MHz) spectra were registered on 400 MHz Agilent, 500 MHz Agilent, or 600 MHz Varian spectrometers. ^{19}F NMR (470 MHz) spectra were obtained on a 500 MHz Agilent spectrometer. ^{1}H NMR and ^{13}C NMR signals were referenced to $CDCl_3$, D_2O, CD_3OD, $(CD_3)_2CO$, or DMSO-d_6 solvent peaks. ^{19}F NMR signals were referenced to an external standard of hexafluorobenzene in $CDCl_3$ (−164.9 ppm). NMR spectroscopy solutions containing NaOD (typically ca. 1 M) were prepared by slowly dissolving NaH in a small amount of the desired solvent under an inert atmosphere, prior to addition of compound.

Mass spectra were obtained on an Agilent ESI-TOF-MS spectrometer operating in positive mode from methanol–acetonitrile solutions containing formic acid as a proton source.

UV-vis absorbance spectra were obtained with an Agilent Cary UV-vis Compact Peltier UV-visible spectrometer. For UV-vis measurements solid samples were dissolved in the desired solvent and diluted as necessary ($\sim 10^{-5}$ mol/L); zwitterionic species were maintained in the solution by addition of TMG (>20 equiv).

Infrared absorption spectra were obtained with a Perkin-Elmer SpectrumOne ATR FT-IR spectrometer in the region of 650 to 4000 cm^{-1}.

X-ray diffraction intensity data were collected on the MX1 beamline at the Australian Synchrotron.[52] The structure was solved by direct methods and difference Fourier synthesis.[53] Thermal ellipsoid plots were generated using the program Mercury integrated within the WINGX suite of programs.[54,55]

Procedures

4-(Pyridin-4-yl)phenol (3)[14]: In a 200 mL Schlenk tube with a magnetic stirrer were added 2.6 g (15 mmol, 1.0 equiv) of 4-bromophenol (**1**), 2.2 g (18 mmol, 1.2 equiv) of 4-pyridinylboronic acid (**2**), 343 mg (0.4 mmol, 2.5 mol%) of tris(dibenzylideneacetone)dipalladium(0) (Pd_2dba_3), 331 mg (0.9 mmol, 6.0 mol%) of tricyclohexylphosphonium tetrafluoroborate ($PCy_3{\cdot}HBF_4$), and 5.4 g (25 mmol, 1.7 equiv) of K_3PO_4. After vacuum/nitrogen cycles, 40 mL of dioxane and 20 mL of distilled water (2/1, v/v) sparged with nitrogen were cannulated. The reaction mixture was stirred at 100 °C for 16 h. The solvents were evaporated from the reaction mixture and the rest was transferred to a separatory funnel with chloroform and water. Excess of 5 mol/L HCl (aq.) was added until the aqueous layer had pH = 0 and precipitate dissolved completely. The mixture was washed with 3 × 150 mL of chloroform and the organic layer was discarded. The aqueous layer was transferred to a larger beaker with a stirrer bar and an aqueous solution of $KHCO_3$ (sat.) was slowly added until pH = 7. A large amount of white solid was formed and then filtered. The product was dried in a vacuum oven and collected as 2.1 g (82%) of yellow solid.

R_f = 0.5 ($CHCl_3$).

IR (solid, cm^{-1}): 2575.7, 1598.9, 1583.4, 1518.9, 1489.5, 1446.2, 1414.8, 1382.8, 1281.6, 1246.4, 1212.5, 1173.1, 1107.8, 1069.4, 1032.4, 1001.7, 894.1, 851.1, 808.7, 728.8, 665.5.

^{1}H NMR (400 MHz, DMSO-d_6) δ: 9.83 (s, 1 H), 8.54 (d, J = 5.8 Hz, 2 H), 7.66 (d, J = 8.6 Hz, 2 H), 7.61 (d, J = 8.6 Hz, 2 H), 6.89 (d, J = 8.6 Hz, 2 H).

^{13}C NMR (101 MHz, CD_3OD) δ: 160.38, 150.57, 150.28, 129.54, 129.33, 122.25, 117.07.

ESI-HRMS: *m*/*z* $[M + H]^+$ calcd for $C_{11}H_{10}NO$: 172.07569; found: 172.07561 (−0.5 ppm error).

4-(4-Hydroxyphenyl)-1-methylpyridinium iodide [OPP(1)-OH][14]: In a 100 mL Schlenk tube with a magnetic stirrer was added 785 mg (4.6 mmol, 1.0 equiv) of 4-(pyridin-4-yl)phenol (**3**). After that 1.14 mL (18.3 mmol, 4.0 equiv) of methyl iodide (MeI) was transferred by a syringe and 70 mL of acetone was cannulated. The reaction mixture

was stirred at 60 °C for 16 h. The solvent was evaporated from the reaction mixture and the residue was washed with Et_2O and EtOAc. The observed pale yellow solid was filtered giving 1.23 g (86%) of yield.

IR (film, cm^{-1}): 3388.2, 3020.9, 1644.4, 1603.7, 1588.5, 1497.5, 1436.2, 1279.2, 1228.7, 1177.2, 827.1.

^1H NMR (400 MHz, CD_3OD) δ: 8.72 (d, J = 6.9 Hz, 2 H), 8.27 (d, J = 6.7 Hz, 2 H), 7.93 (d, J = 8.5 Hz, 2 H), 7.00 (d, J = 8.4 Hz, 2 H), 4.32 (s, 3 H).

^{13}C NMR (101 MHz, CD_3OD) δ: 163.82, 157.15, 146.07, 131.14, 125.40, 123.97, 117.91, 47.54.

ESI-HRMS: m/z $[M - I^-]^+$ calcd for $C_{12}H_{12}NO$: 186.09134; found: 186.09151 (+0.9 ppm error).

4-(1-Methylpyridinium-4-yl)phenolate [OPP(1)-O$^-$][14]: In a 20 mL microwave vial with a magnetic stirrer was added 200 mg (0.64 mmol, 1.0 equiv) of 4-(4-hydroxyphenyl)-1-methylpyridinium iodide [**OPP(1)-OH**]. The vial was capped and 4 mL of MeOH was transferred followed by addition 0.8 mL (0.8 mmol, 1.3 equiv) of tetrabutylammonium hydroxide (NBu_4OH, 1 mol/L solution in MeOH). The reaction mixture was stirred at r.t. for 15 min. The formed orange precipitate was filtered and washed with DCM/Et_2O (1/1, v/v). After drying in a vacuum oven overnight, 110 mg (93%) of orange solid was obtained.

IR (film, cm^{-1}): 3445, 1643.9, 1568.4, 1486.8, 1307.2, 1202.3, 1168.7, 827.9, 686.5.

^1H NMR (600 MHz, DMSO-d_6) δ: 8.48 (d, J = 7.0 Hz, 2 H), 8.04 (d, J = 7.2 Hz, 2 H), 7.80 (d, J = 9.0 Hz, 2 H), 6.56 (d, J = 9.0 Hz, 2 H), 4.08 (s, 3 H). ^1H NMR (600 MHz, D_2O, NaOD) δ: 7.80 (d, J = 6.7 Hz, 2 H), 7.34 (d, J = 7.1 Hz, 2 H), 7.23 (d, J = 8.9 Hz, 2 H), 6.39 (d, J = 8.8 Hz, 2 H), 3.77 (s, 3 H). ^1H NMR (600 MHz, CD_3OD, NaOD) δ: 8.33 (d, J = 6.9 Hz, 2 H), 7.92 (d, J = 5.3 Hz, 2 H), 7.70 (d, J = 9.2 Hz, 2 H), 6.61 (d, J = 8.9 Hz, 2 H), 4.13 (s, 3 H).

^{13}C NMR (151 MHz, CD_3OD, NaOD) δ: 177.18, 156.71, 144.27, 131.25, 121.91, 120.76, 117.56, 46.46.

ESI-HRMS: m/z $[M + H]^+$ calcd for $C_{12}H_{12}NO$: 186.09134; found: 186.09147 (+0.7 ppm error).

1-(Benzyloxy)-4-bromobenzene (4)[56]: In a 100 mL round-bottom flask (RBF) with a magnetic stirrer were transferred 2.0 g (11.5 mmol, 1.0 equiv) of 4-bromophenol (**1**), 4.8 g (34.6 mmol, 3.0 equiv) of K_2CO_3, and 0.19 g (1.15 mmol, 10 mol%) of KI. The RBF was equipped with a condenser and 50 mL of acetone was cannulated. After that 1.46 mL (12.7 mmol, 1.1 equiv) of BnCl was transferred by a syringe. The reaction mixture was stirred at 60°C for 16 h and after completion transferred to a separatory funnel with 15 mL of EtOAc. The reaction mixture was washed with 5 × 15 mL of water. The organic layer was dried with $MgSO_4$ and filtered. The solvent was removed by rotary evaporation giving 3.1 g (98%) of colorless oil, which was dried in a vacuum oven and used in the next step without any further purification.

R_f = 0.24 (petroleum spirits).

IR (film, cm^{-1}): 3524.2, 3032.2, 1589.1, 1486.8, 1453.8, 1381.3, 1285.5, 1239.2, 1171.2, 1102.5, 1072, 1002.1, 820.6, 734.6, 696.8.

^1H NMR (500 MHz, $CDCl_3$) δ: 7.48–7.35 (m, 7 H), 6.89 (d, J = 8.6 Hz, 2 H), 5.06 (s, 2 H).

^{13}C NMR (126 MHz, $CDCl_3$) δ: 157.90, 136.59, 132.36, 128.72, 128.19, 127.53, 116.75, 113.18, 70.24.

ESI-HRMS: m/z $[M]^{\bullet+}$ calcd for $C_{13}H_{11}BrO$: 261.99878; found: 261.99839 (−1.5 ppm error).

4′-(Benzyloxy)-[1,1′-biphenyl]-4-ol (6)[57]: In a 100 mL Schlenk tube with a magnetic stirrer were added 2.0 g (7.6 mmol, 1.0 equiv) of 1-(benzyloxy)-4-bromobenzene (**4**), 1.25 g (9.12 mmol, 1.2 equiv) of (4-hydroxyphenyl) boronic acid (**5**), 34.8 mg (0.04 mmol, 0.5 mol%) of Pd_2dba_3, 33.6 mg (0.09 mmol, 1.2 mol%) of $PCy_3{\cdot}HBF_4$, and 2.4 g (11.4 mmol, 1.5 equiv) of K_3PO_4. After vacuum/nitrogen cycles, 20 mL of dioxane and 10 mL of distilled water (2/1, v/v) sparged with nitrogen were cannulated. The reaction mixture was stirred at 100 °C for 16 h. The solvents were evaporated from the reaction mixture and the rest was transferred to a separatory funnel with EtOAc and water. The mixture was washed with 2 × 50 mL of NH_4Cl (sat.) aqueous solution until pH = 7 and 2 × 50 mL of water and the aqueous layer was discarded. The organic layer was collected, dried with $MgSO_4$, and filtered. The solvent was removed by rotary evaporation and the crude product was filtered through a small silica gel plug using hot EtOAc. The solvent was removed under reduced pressure and the product was recrystallized from toluene. After filtration and drying in a vacuum oven, 1.56 g (70%) of white solid was obtained.

R_f = 0.22 ($CHCl_3$:toluene 2:1).

IR (film, cm^{-1}): 3438.1, 3048.3, 3035, 2907.7, 2866.2, 1610.5, 1596.8, 1500.1, 1470, 1454.1, 1408.9, 1375, 1315, 1302.5, 1282.9, 1263.6, 1247.4, 1192.1, 1176.4, 1134.6, 1082.6, 1027.2, 1008.9, 918.7, 862.9, 837.8, 813, 746, 699.8.

^1H NMR (500 MHz, $(CD_3)_2CO$) δ: 8.35 (s, 1 H), 7.52–7.48 (m, 5 H), 7.44 (d, J = 8.6 Hz, 2 H), 7.40 (t, J = 7.7, 7.1 Hz, 2 H), 7.33 (t, J = 7.5 Hz, 1 H), 7.06 (d, J = 8.8 Hz, 2 H), 6.90 (d, J = 8.7 Hz, 2 H), 5.15 (s, 2 H).

^{13}C NMR (126 MHz, $(CD_3)_2CO$) δ: 158.76, 157.48, 138.49, 134.63, 132.93, 129.28, 128.59, 128.39, 128.37, 128.16, 116.47, 115.98, 70.48.

ESI-MS (positive mode): m/z $[M]^{\bullet+}$ calcd for $C_{19}H_{16}O_2$: 276.11448; found: 276.11438 (−0.4 ppm error).

4′-(Benzyloxy)-[1,1′-biphenyl]-4-yl 1,1,2,2,3,3,4,4,4-nonafluorobutane-1-sulfonate (7): In a 100 mL Schlenk tube with a magnetic stirrer was added 1.0 g (3.6 mmol, 1.0 equiv) of 4′-(benzyloxy)-[1,1′-biphenyl]-4-ol (**6**). After vacuum/nitrogen cycles, 30 mL of anhydrous DCM was cannulated and 0.75 mL (5.4 mmol, 1.5 equiv) of anhydrous Et_3N was transferred by a syringe. The reaction mixture was stirred and cooled to 0 °C followed by

addition of 0.77 mL (4.3 mmol, 1.2 equiv) of NfF dropwise by a syringe. The reaction mixture was stirred at r.t. for 16 h. After completion, the reaction mixture was diluted with an equal amount (30 mL) of petroleum spirits and filtered through a small silica gel plug using petroleum spirits:DCM 1:1 mixture. The solvents were removed under reduced pressure and the final product was obtained after drying in a vacuum oven as 1.97 g (98%) of white solid.

R_f = 0.2 (petroleum spirits:DCM 5:1).

IR (film, cm^{-1}): 3038.8, 2897, 2859.2, 1610, 1597.1, 1571.1, 1493, 1468.5, 1456.5, 1432.4, 1385.2, 1354.4, 1291.7, 1244.6, 1199.7, 1140.1, 1123.2, 1106.2, 1033.8, 1016.4, 1002.1, 943.7, 890.1, 848.4, 837.7, 813.8, 766, 743.8, 732, 697.6, 674.6.

^{1}H NMR (500 MHz, $CDCl_3$) δ: 7.59 (d, J = 8.8 Hz, 2 H), 7.49 (d, J = 8.8 Hz, 2 H), 7.46 (d, J = 7.3 Hz, 2 H), 7.41 (t, J = 7.6 Hz, 2 H), 7.39–7.30 (m, 3 H), 7.07 (d, J = 8.8 Hz, 2H), 5.12 (s, 1 H).

^{13}C NMR (126 MHz, $CDCl_3$) δ: 159.01, 148.87, 141.34, 136.86, 132.12, 128.79, 128.45, 128.42, 128.23, 127.62, 121.73, 115.46, 70.23.

^{19}F NMR (470 MHz, $CDCl_3$) δ: −80.61, −108.92, −120.85, −125.79.

ESI-HRMS: m/z $[M]^{\bullet+}$ calcd for $C_{23}H_{15}F_9O_4S$: 558.05418; found: 558.05481 (+0.1 ppm error).

4″-(Benzyloxy)-[1,1′:4′,1″-terphenyl]-4-ol (8): In a 100 mL Schlenk tube with a magnetic stirrer were added 1.0 g (1.7 mmol, 1.0 equiv) of 4′-(benzyloxy)-[1,1′-biphenyl]-4-yl 1,1,2,2,3,3,4,4,4-nonafluorobutane-1-sulfonate (**7**), 1.3 g (2.1 mmol, 1.2 equiv) of (4-hydroxyphenyl)boronic acid (**5**), 7.8 mg (8.5 µmol, 0.5 mol%) of Pd_2dba_3, 7.5 mg (20.4 µmol, 1.2 mol%) of $PCy_3{\cdot}HBF_4$, and 0.6 g (2.9 mmol, 1.7 equiv) of K_3PO_4. After vacuum/nitrogen cycles, 20 mL of dioxane and 10 mL of distilled water (2/1, v/v) sparged with nitrogen were cannulated. The reaction mixture was stirred at 100 °C for 16 h. After completion, 10 mL of MeOH and 10 mL of water were added to the reaction mixture and the crude product was filtered and washed with 3 × 20 mL of hot $CHCl_3$ (to remove unreacted starting material) and 3 × 20 mL of MeOH and water. After drying in a vacuum oven, 336 mg (56%) of gray solid was collected. As the product was poorly soluble in most organic solvents, it was used in the next step without any further purification.

IR (solid, cm^{-1}): 3430.8, 3064.8, 3035.2, 2907.2, 2865.9, 1606.7, 1596.4, 1580.7, 1558.4, 1536.5, 1490.4, 1468.6, 1454.6, 1447.9, 1420, 1401.7, 1376.6, 1315.9, 1285, 1261.1, 1246.4, 1181.1, 1144.1, 1110.4, 1084.6, 1036.1, 1020.1, 1007.9, 998.2, 918, 861.1, 829.7, 808.5, 755.4, 737.4, 713.2, 697.6, 678.3, 661.3.

^{1}H NMR (500 MHz, DMSO-d_6) δ: 9.57 (s, 1 H), 7.68–7.61 (m, 6 H), 7.52 (d, J = 8.6 Hz, 2 H), 7.47 (d, J = 7.0 Hz, 2 H), 7.41 (t, J = 7.5 Hz, 2 H), 7.34 (t, J = 7.3 Hz, 1 H), 5.16 (s, 2 H).

^{13}C NMR (126 MHz, DMSO-d_6) δ: 157.90, 157.16, 138.51, 137.64, 137.08, 132.30, 130.35, 128.44, 127.82, 127.64, 127.53, 127.50, 126.50, 126.31, 115.75, 115.27, 69.24.

ESI-HRMS: m/z $[M]^{\bullet+}$ calcd for $C_{25}H_{20}O_2$: 352.14578; found: 352.14591 (+0.4 ppm error).

4″-(Benzyloxy)-[1,1′:4′,1″-terphenyl]-4-yl 1,1,2,2,3,3,4,4,4-nona-fluorobutane-1-sulfonate (9): In a 100 mL Schlenk tube with a magnetic stirrer was added 200 mg (0.57 mmol, 1.0 equiv) of4″-(benzyloxy)-[1,1′:4′,1″-terphenyl]-4-ol (**8**). After vacuum/nitrogen cycles, 20 mL of anhydrous DMF was cannulated and 0.12 mL (0.85 mmol, 1.5 equiv) of anhydrous Et_3N was transferred by a syringe. The reaction mixture was stirred and cooled to 0 °C followed by addition of 0.12 mL (0.68 mmol, 1.2 equiv) of NfF dropwise by a syringe. After that, the reaction mixture was stirred at 60 °C for 16 h. After completion, the reaction mixture was evaporated and filtered through a small silica gel plug using toluene:DCM (1:1, v/v) mixture. The solvents were removed under reduced pressure and the final product was obtained after drying in a vacuum oven as 340 mg (94%) of white solid.

R_f = 0.96 (toluene:DCM 1:1).

IR (film, cm^{-1}): 1603.9, 1489.3, 1431.2, 1354.3, 1291.3, 1198, 1141.4, 1036.3, 1016, 885.8, 811.1, 776, 731.9, 695.4.

^{1}H NMR (500 MHz, $CDCl_3$) δ: 7.68 (d, J = 8.8 Hz, 2 H), 7.65 (d, J = 8.6 Hz, 2 H), 7.61 (d, J = 8.5 Hz, 2 H), 7.58 (d, J = 8.7 Hz, 2 H), 7.47 (d, J = 7.1 Hz, 2 H), 7.41 (t, J = 7.4 Hz, 2 H), 7.38–7.33 (m, 3 H), 7.08 (d, J = 8.7 Hz, 2 H), 5.13 (s, 2 H).

^{13}C NMR (126 MHz, $CDCl_3$) δ: 158.60, 149.11, 141.21, 140.50, 137.50, 136.86, 133.05, 128.65, 128.10, 128.05, 127.51, 127.49, 127.22, 121.68, 115.24, 70.10, 29.72.

^{19}F NMR (470 MHz, $CDCl_3$) δ: −80.59, −108.86, −120.85, −125.80.

ESI-HRMS: m/z $[M]^{\bullet+}$ calcd for $C_{29}H_{19}F_9O_4S$: 634.08549; found: 634.08525 (−0.4 ppm error).

4-(4′-(Benzyloxy)-[1,1′-biphenyl]-4-yl)pyridine (10): In a 100 mL Schlenk tube with a magnetic stirrer were added 2.5 g (4.4 mmol, 1.0 equiv) of 4′-(benzyloxy)-[1,1′-biphenyl]-4-yl 1,1,2,2,3,3,4,4,4-nonafluorobutane-1-sulfonate (**7**), 0.66 g (5.3 mmol, 1.2 equiv) of 4-pyridinylboronic acid, 20.1 mg (0.022 mmol, 0.5 mol%) of Pd_2dba_3, 19.4 mg (0.053 mmol, 1.2 mol%) of $PCy_3{\cdot}HBF_4$, and 1.58 g (7.48 mmol, 1.7 equiv) of K_3PO_4. The tube was capped and after vacuum/nitrogen cycles, 50 mL of dioxane and 25 mL of distilled water (2/1, v/v) sparged with nitrogen were cannulated. The reaction mixture was stirred at 100 °C for 16 h. After completion, the crude product was filtered and washed with 3 × 250 mL of MeOH and water. After that solid was dissolved in $CDCl_3$ and loaded onto silica, then eluted through a silica gel plug using EtOAc:DCM (1:1, v/v) mixture. The solvents were removed under reduced pressure and the final product was obtained after drying in a vacuum

oven as 1.05 g (70%) of white solid. The obtained compound is poorly soluble in most organic solvents.

R_f = 0.36 (EtOAc:DCM 1:1).

IR (film, cm^{-1}): 3038, 2923.4, 2854.4, 1540.3, 1508, 1486.8, 1460.6, 1450.9, 1409.3, 1379.8, 1290.3, 1254.8, 1230.7, 1210.6, 1181.9, 1117.6, 1045.9, 1028.4, 1000.3, 833.1, 805.1, 735.1, 696.1.

^{1}H NMR (500 MHz, $CDCl_3$) δ: 8.67 (d, J = 6.1 Hz, 2 H), 7.71 (d, J = 8.5 Hz, 2 H), 7.68 (d, J = 8.4 Hz, 2 H), 7.58 (d, J = 8.8 Hz, 2 H), 7.55 (d, J = 6.0 Hz, 2 H), 7.47 (d, J = 7.2 Hz, 2 H), 7.41 (t, J = 7.4 Hz, 2 H), 7.35 (t, J = 7.2 Hz, 1 H), 7.08 (d, J = 8.6 Hz, 2 H), 5.13 (s, 2 H).

^{13}C NMR (151 MHz, $CDCl_3$) δ: 158.92, 149.98, 148.44, 141.86, 136.99, 136.22, 133.01, 128.79, 128.30, 128.20, 127.62, 127.52, 127.50, 121.63, 115.46, 70.28.

ESI-HRMS: *m/z* $[M + H]^+$ calcd for $C_{24}H_{20}NO$: 338.15394; found: 338.15472 (+0.2 ppm error).

4-(4″-(Benzyloxy)-[1,1′:4′,1″-terphenyl]-4-yl)pyridine (11): In 3 × 20 mL microwave vials with a magnetic stirrer each were added 500 mg (0.79 mmol, 1.0 equiv) of 4″-(benzyloxy)-[1,1′:4′,1″-terphenyl]-4-yl 1,1,2,2,3,3,4,4,4-nonafluorobutane-1-sulfonate (**9**), 194 mg (1.6 mmol, 2.0 equiv) of 4-pyridinylboronic acid, 18.0 mg (0.02 mmol, 2.5 mol%) of Pd_2dba_3, 17.4 mg of $PCy_3{\cdot}HBF_4$ (0.05 mmol, 6.0 mol%), and 284.3 mg (1.34 mmol, 1.7 equiv) of K_3PO_4. The vial was capped and after vacuum/nitrogen cycles, 12.5 mL of THF and 1.25 mL of distilled water (10/1, v/v) sparged with nitrogen were cannulated. The reaction mixture was stirred at 100°C for 48 h. After completion, the reaction mixtures were joined and the crude product was filtered and washed with 3 × 60 mL of MeOH and water. After that, the crude product was loaded onto silica and purified by Soxhlet extraction with hot $CHCl_3$. After 2 days, white solid crashed out in the collection flask. The formed product was filtered and washed with $CHCl_3$. After drying under high vacuum overnight, 585 mg (60%) of white solid was obtained. The compound is almost insoluble in most organic solvents.

IR (solid, cm^{-1}): 3059.7, 3037.2, 2883.8, 2855.5, 1591, 1582, 1557.7, 1539.5, 1497.2, 1483.8, 1459.7, 1451.4, 1415.3, 1403.7, 1377.1, 1338.5, 1317.1, 1289.4, 1267.6, 1249.2, 1231.8, 1220.5, 1205, 1178.1, 1153.4, 1116.2, 1079.1, 1044.8, 1026.8, 999.9, 990.4, 909.5, 852.4, 824.8, 802.6, 730.5, 696.6, 667.6.

^{1}H NMR (600 MHz, $CDCl_3$, 60 °C) δ: 8.72 (d, J = 5.3 Hz, 2 H), 7.81 (q, J = 8.2 Hz, 6 H), 7.71 (d, J = 8.6 Hz, 2 H), 7.68 (d, J = 7.6 Hz, 2 H), 7.59 (d, J = 8.7 Hz, 2 H), 7.47 (d, J = 7.6 Hz, 2 H), 7.41 (t, J = 7.4 Hz, 2 H), 7.34 (t, J = 7.4 Hz, 1 H), 7.09 (d, J = 8.7 Hz, 2 H), 5.14 (s, 2 H).

ESI-HRMS: *m/z* $[M + H]^+$ calcd for $C_{30}H_{24}NO$: 414.18524; found: 414.18522 (−0.1 ppm error).

4-(4′-(Benzyloxy)-[1,1′-biphenyl]-4-yl)-1-methylpyridinium iodide (12): In a 20 mL microwave vial with a magnetic stirrer was added 300 mg (0.89 mmol, 1.0 equiv) of 4-(4′-(benzyloxy)-[1,1′-biphenyl]-4-yl)pyridine (**10**). The vial was capped and 15 mL of anhydrous DMF was cannulated followed by 0.3 mL (4.8 mmol, 5.5 equiv) of MeI. The reaction mixture was stirred at 60 °C for 48 h. After completion, a large amount of yellow solid was formed. To the reaction mixture 30 mL of diethyl ether was added and shook well. The product was filtered and dried under high vacuum at 100 °C overnight. The product was collected as 418 mg (98%) of yellow solid.

IR (solid, cm^{-1}): 3014, 2934.7, 2872, 1909.2, 1638.2, 1592.6, 1579.2, 1539.9, 1490.5, 1466.1, 1458.1, 1406.2, 1382.3, 1345.8, 1329.2, 1287, 1248.2, 1230.3, 1208, 1187.5, 1111.2, 1084.4, 1052.9, 1019.8, 1008.3, 996.4, 966.6, 944.7, 930.2, 867.9, 836.3, 813.7, 771.8, 742.1, 714.7, 703.3, 661.2.

^{1}H NMR (600 MHz, CD_3OD) δ: 8.85 (d, J = 7.0 Hz, 2 H), 8.42 (d, J = 7.0 Hz, 2 H), 8.08 (d, J = 8.5 Hz, 2 H), 7.88 (d, J = 8.5 Hz, 2 H), 7.69 (d, J = 8.8 Hz, 2 H), 7.47 (d, J = 6.9 Hz, 2 H), 7.39 (t, J = 7.6 Hz, 2 H), 7.32 (t, J = 7.3 Hz, 1 H), 7.14 (d, J = 8.8 Hz, 2 H), 5.17 (s, 2 H), 4.39 (s, 3 H). ^{1}H NMR (600 MHz, DMSO-d_6) δ: 8.98 (d, J = 6.9 Hz, 2 H), 8.53 (d, J = 9.2 Hz, 2 H), 8.16 (d, J = 8.5 Hz, 2 H), 7.91 (d, J = 8.6 Hz, 2 H), 7.77 (d, J = 8.7 Hz, 2 H), 7.48 (d, J = 7.8 Hz, 2 H), 7.41 (t, J = 7.6 Hz, 2 H), 7.34 (t, J = 7.4 Hz, 1 H), 7.16 (d, J = 8.8 Hz, 2 H), 5.19 (s, 2 H), 4.33 (s, 3 H).

^{13}C NMR (151 MHz, DMSO-d_6) δ: 158.83, 153.70, 145.49, 143.21, 136.95, 131.50, 130.96, 128.68, 128.50, 128.19, 127.91, 127.69, 127.13, 123.64, 115.49, 69.33, 47.01.

ESI-HRMS: *m/z* $[M\text{-}I^-]^+$ calcd for $C_{25}H_{22}NO$: 352.16959; found: 352.16976 (0.5 ppm error).

4-(4″-(Benzyloxy)-[1,1′:4′,1″-terphenyl]-4-yl)-1-methylpyridinium iodide (13): In a 25 mL microwave vial with a magnetic stirrer was added 300 mg (0.73 mmol, 1.0 equiv) of 4-(4″-(benzyloxy)-[1,1′:4′,1″-terphenyl]-4-yl) pyridine (**11**). The vial was capped and 15 mL of anhydrous DMF was cannulated followed by transferring 0.2 mL (3.2 mmol, 4.4 equiv) of MeI. The reaction mixture was stirred at 100 °C for 48 h. After completion, a large amount of yellow solid was formed. To the reaction mixture, 30 mL of diethyl ether was added and shook well. The product was filtered and dried under high vacuum at 100 °C overnight. The product was collected as 394 mg (98%) of yellow solid.

IR (solid, cm^{-1}): 2993.7, 1637.4, 1597.1, 1580.6, 1560.6, 1525.7, 1487.7, 1470.3, 1459.3, 1450.9, 1427.3, 1402.6, 1378.8, 1341.1, 1315.8, 1290.5, 1251.3, 1231, 1219, 1199.2, 1185.5, 1178.4, 1163.9, 1116, 1040, 1026.7, 998.7, 944.8, 847.2, 834.6, 814.1, 806, 768.5, 745.2, 723.7, 716.3, 697.4.

^{1}H NMR (600 MHz, DMSO-d_6) δ: 9.01 (d, J = 7.0 Hz, 2 H), 8.57 (d, J = 7.1 Hz, 2 H), 8.21 (d, J = 8.5 Hz, 2 H), 8.02 (d, J = 8.6 Hz, 2 H), 7.89 (d, J = 8.4 Hz, 2 H), 7.78 (d, J = 8.5 Hz, 2 H), 7.70 (d, J = 8.8 Hz, 2 H), 7.48 (d, J = 6.8 Hz, 2 H), 7.41 (t, J = 7.6 Hz, 2 H), 7.35 (t, J = 7.3 Hz, 1 H), 7.14 (d, J = 8.9 Hz, 2 H), 5.18 (s, 2 H), 4.34 (s, 3 H).

^{13}C NMR (151 MHz, DMSO-d_6) δ: 158.25, 153.65, 145.54, 143.06, 139.81, 137.03, 136.71, 132.22, 131.86, 128.74,

128.47, 127.78, 127.66, 127.52, 127.40, 126.80, 123.77, 115.35, 69.27, 54.40.

ESI-HRMS: *m*/*z* [M-I$^-$]$^+$ calcd for $C_{31}H_{26}NO$: 428.20089. Found: 428.20076 (−0.3 ppm error).

4-(4′-Hydroxy-[1,1′-biphenyl]-4-yl)-1-methylpyridinium chloride [OPP(2)-OH]: In a 20 mL microwave vial with a magnetic stirrer were added 190 mg (0.4 mmol, 1.0 equiv) of 4-(4′-(benzyloxy)-[1,1′-biphenyl]-4-yl)-1-methylpyridinium iodide (**12**) and 10 mL (large excess) of hydrobromic acid solution (33 wt% in acetic acid). The vial was capped and the reaction mixture was stirred at r.t. for 16 h. Conversion of benzyl group to the acetate functionality was confirmed by ESI-MS [positive mode; calculated *m*/*z* for [M]$^+$: 304.13321, found: 304.13299 (−0.3 ppm error)]. After completion, the reaction mixture was dried under nitrogen flow and washed thoroughly with centrifugation using 3 × 40 mL of DCM, 2 × 5 mL of 1 mol/L aqueous sodium metabisulfite solution, and 10 mL of water. The obtained solid was transferred to a 20 mL microwave vial with a magnetic stirrer followed by addition of 8 mL of MeOH and 1.5 mL of 32% aqueous HCl. The vial was capped and the reaction mixture was stirred at 60 °C for 16 h. After completion, the reaction mixture was dried under nitrogen flow and washed consistently by centrifugation with 10 mL of water and 5 mL of 1 M sodium metabisulfite solution. To the obtained solid was added 1 mL (excess) of 1 mol/L NaOH solution to ensure complete deprotonation and the mixture was sonicated. After discarding the excess of the base, the solid was treated with 1 mL of 1 mol/L HCl solution. After sonication excess of the acid was discarded, the solid was washed with 10 mL of water and dried. After drying in a vacuum oven overnight, 40 mg (35%) of yellow solid was obtained.

IR (film, cm^{-1}): 3393.8, 2966.8, 1644.1, 1601.8, 1541, 1494.8, 1274.8, 1231.7, 1191.2, 1054.7, 1033.3, 813.1.

^{1}H NMR (600 MHz, DMSO-d_6) δ: 9.77 (s, 1 H), 8.99 (d, J = 6.3 Hz, 2 H), 8.54 (d, J = 6.3 Hz, 2 H), 8.14 (d, J = 8.1 Hz, 2 H), 7.87 (d, J = 8.1 Hz, 2 H), 7.66 (d, J = 8.2 Hz, 2 H), 6.90 (d, J = 8.2 Hz, 2 H), 4.32 (s, 3 H). ^{1}H NMR (600 MHz, CD_3OD) δ: 8.84 (d, J = 6.9 Hz, 2 H), 8.40 (d, J = 6.9 Hz, 2 H), 8.06 (d, J = 8.6 Hz, 2 H), 7.84 (d, J = 8.5 Hz, 2 H), 7.60 (d, J = 8.7 Hz, 2 H), 6.91 (d, J = 8.6 Hz, 2 H), 4.39 (s, 3 H).

^{13}C NMR (151 MHz, CD_3OD) δ: 159.46, 157.13, 146.48, 146.43, 132.65, 131.61, 129.59, 129.32, 128.49, 125.18, 116.97, 47.88.

ESI-HRMS: *m*/*z* [M − Cl$^-$]$^+$ calcd for $C_{18}H_{16}NO$: 262.12264; found: 262.12249 (−0.6 ppm error).

4′-(1-Methylpyridin-1-ium-4-yl)-[1,1′-biphenyl]-4-olate [OPP(2)-O$^-$]: In a 15 mL centrifuge vial, 20 mg (0.04 mmol, 1 equiv) of 4-(4′-hydroxy-[1,1′-biphenyl]-4-yl)-1-methylpyridinium chloride [**OPP(2)-OH**] and 1 mL (1 mmol, 25 equiv) of 1 mol/L NaOH solution were added. After sonication and centrifugation, excess of the base was discarded and the solid was washed with 5 mL of water and dried. After drying in a vacuum oven overnight, 17.2 mg (98%) of red solid was obtained.

IR (solid, cm^{-1}): 3056.3, 1644.6, 1575.9, 1539.6, 1487.7, 1424.2, 1328.5, 1284.8, 1233.2, 1188, 1171.3, 1110.4, 989.6, 879.1, 851.5, 817.4, 743.7, 721.6.

^{1}H NMR (600 MHz, DMSO-d_6) δ: 8.83 (d, J = 6.5 Hz, 2 H), 8.40 (d, J = 6.6 Hz, 2 H), 8.01 (d, J = 8.5 Hz, 2 H), 7.73 (d, J = 8.2 Hz, 2 H), 7.45 (d, J = 8.5 Hz, 2 H), 6.46–6.41 (m, 2 H), 4.28 (s, 3 H). ^{1}H NMR (600 MHz, CD_3OD) δ: 8.63 (d, J = 6.9 Hz, 2 H), 8.18 (d, J = 7.0 Hz, 2 H), 7.84 (d, J = 8.6 Hz, 2 H), 7.65 (d, J = 8.6 Hz, 2 H), 7.39 (d, J = 8.7 Hz, 2 H), 6.66 (d, J = 8.6 Hz, 2 H), 4.28 (s, 3 H).

ESI-HRMS: *m*/*z* [M + H]$^+$ calcd for $C_{18}H_{16}NO$: 262.12264; found: 262.12266 (+0.1 ppm error).

4-(4″-Hydroxy-[1,1′:4′,1″-terphenyl]-4-yl)-1-methylpyridinium chloride [OPP(3)-OH]: In a 20 mL microwave vial with a magnetic stirrer were added 230 mg (0.4 mmol, 1.0 equiv) of 4-(4″-(benzyloxy)-[1,1′:4′,1″-terphenyl]-4-yl)-1-methylpyridinium iodide (**13**) and 15 mL (large excess) of hydrobromic acid solution (33 wt% in acetic acid). The vial was capped and the reaction mixture was stirred at r.t. for 16 h. Conversion of benzyl group to the acetate functionality was confirmed by ESI-MS [positive mode; calculated *m*/*z* for [M] + : 380.16451, found: 380.16458 (0.2 ppm error)]. After completion, the reaction mixture was dried under nitrogen flow and washed consistently by centrifugation with 3 × 40 mL of DCM, 2 × 5 mL of 1 mol/L sodium metabisulfite solution, and 10 mL of water. The obtained solid was transferred to a 20 mL microwave vial with a magnetic stirrer followed by addition of 15 mL of MeOH and 1.5 mL of 32% aqueous HCl. The vial was capped and the reaction mixture was stirred at 60 °C for 16 h. After completion, the reaction mixture was dried under nitrogen flow and washed thoroughly with centrifugation using 10 mL of water and 5 mL of 1 M sodium metabisulfite solution. To the obtained solid was added 1 mL (excess) of 1 mol/L NaOH solution to ensure complete deprotonation and the mixture was sonicated. After discarding the excess of the base, the solid was treated with 1 mL of 1 mol/L HCl solution. After sonication excess of the acid was discarded, the solid was washed with 10 mL of water and dried. After drying in a vacuum oven overnight, 114 mg (76%) of yellow solid was obtained.

IR (solid, cm^{-1}): 3365.3, 3035.1, 2586.3, 1916.9, 1640, 1597.3, 1526.3, 1488.5, 1401.4, 1343.1, 1278.4, 1222.4, 1199.4, 1173.4, 1108.4, 1044.8, 1000.4, 851, 808.7, 768.3, 728.3, 710.4.

^{1}H NMR (600 MHz, DMSO-d_6) δ: 9.02 (d, J = 6.4 Hz, 2 H), 8.57 (d, J = 6.9 Hz, 2 H), 8.20 (d, J = 8.5 Hz, 2 H), 8.00 (d, J = 8.4 Hz, 2 H), 7.87 (d, J = 8.4 Hz, 2 H), 7.74 (d, J = 8.4 Hz, 2 H), 7.58 (d, J = 8.5 Hz, 2 H), 6.89 (d, J = 8.5 Hz, 2 H), 4.34 (s, 3 H).

^{13}C NMR (151 MHz, DMSO-d_6) δ: 157.45, 153.64, 145.53, 143.11, 140.25, 136.27, 132.11, 129.99, 128.72, 127.73, 127.44, 127.32, 126.52, 123.73, 115.82, 47.00.

ESI-HRMS: m/z $[M\text{-}Cl^-]^+$ calcd for $C_{24}H_{20}NO$: 338.15394; found: 338.15373 (−0.6 ppm error).

4″-(1-Methylpyridin-1-ium-4-yl)-[1,1′:4′,1″-terphenyl]-4-olate [OPP(3)-O$^-$]: In a 15 mL centrifuge vial, 20 mg (0.05 mmol, 1 equiv) of 4-(4″-hydroxy-[1,1′:4′,1″-terphenyl]-4-yl)-1-methylpyridinium chloride [**OPP(3)-OH**] and 1 mL (1 mmol, 20 equiv) of 1 mol/L NaOH solution were added. After sonication and centrifugation, excess of the base was discarded and the solid was washed with 5 mL of water and dried. After drying in a vacuum oven overnight, 16.7 mg (93%) of purple solid was obtained.

IR (solid, cm^{-1}): 3049.8, 2276.1, 1642.2, 1574.8, 1525.2, 1504.7, 1483.8, 1403.9, 1319.7, 1301.9, 1280.4, 1234.8, 1223.1, 1203.2, 1186.8, 1171.9, 1108.2, 989.9, 880.3, 845.8, 811, 768.9, 728.2.

ESI-HRMS: m/z $[M + H]^+$ calcd for $C_{24}H_{20}NO$: 338.15394; found: 338.15396 (+0.1 ppm error).

Funding Information

This work was funded by the Australian Research Council through the ARC Centre of Excellence in Exciton Science (CE170100026).

Acknowledgment

IZ and TCO thank the University of Melbourne for scholarship support. We gratefully acknowledge the Australian Synchrotron for beamtime via the Collaborative Access Program (proposal number 13618b). The authors acknowledge access to the Mass Spectrometry and Proteomics Facility (MSPF) at the Bio21 Institute, University of Melbourne.

Supporting Information

Supporting Information for this article is available online at https://doi.org/10.1055/s-0041-1725075.

References

(1) Fort, A.; Boeglin, A.; Mager, L.; Amyot, C.; Combellas, C.; Thiébault, A.; Rodriguez, V. *Synth. Met.* **2001**, *124*, 209.
(2) Boeglin, A.; Fort, A.; Mager, L.; Combellas, C.; Thiébault, A.; Rodriguez, V. *Chem. Phys.* **2002**, *282*, 353.
(3) Reichardt, C. *Chem. Rev.* **1994**, *94*, 2319.
(4) He, G. S.; Zhu, J.; Baev, A.; Samoć, M.; Frattarelli, D. L.; Watanabe, N.; Facchetti, A.; Ågren, H.; Marks, T. J.; Prasad, P. N. *J. Am. Chem. Soc.* **2011**, *133*, 6675.
(5) Marder, S. R.; Kippelen, B.; Jen, A. K.-Y.; Peyghambarian, N. *Nature* **1997**, *388*, 845.
(6) Diemer, V.; Chaumeil, H.; Defoin, A.; Fort, A.; Boeglin, A.; Carré, C. *Eur. J. Org. Chem.* **2006**, 2727.
(7) Shi, Y.; Frattarelli, D.; Watanabe, N.; Facchetti, A.; Cariati, E.; Righetto, S.; Tordin, E.; Zuccaccia, C.; Macchioni, A.; Wegener, S. L.; Stern, C. L.; Ratner, M. A.; Marks, T. J. *J. Am. Chem. Soc.* **2015**, *137*, 12521.
(8) Yamaguchi, I.; Yamaji, R. *J. Phys. Org. Chem.* **2017**, *30*, e3671.
(9) Yamaguchi, I.; Goto, K.; Sato, M. *Tetrahedron* **2009**, *65*, 3645.
(10) Brooker, L.; Keyes, G.; Heseltine, D. *J. Am. Chem. Soc.* **1951**, *73*, 5350.
(11) Morley, J. O.; Morley, R. M.; Docherty, R.; Charlton, M. H. *J. Am. Chem. Soc.* **1997**, *119*, 10192.
(12) Rezende, M. C. *J. Phys. Org. Chem.* **2016**, *29*, 460.
(13) Catalan, J.; Mena, E.; Meutermans, W.; Elguero, J. *J. Phys. Chem.* **1992**, *96*, 3615.
(14) Diemer, V.; Chaumeil, H.; Defoin, A.; Jacques, P.; Carré, C. *Tetrahedron Lett.* **2005**, *46*, 4737.
(15) Machado, V. G.; Stock, R. I.; Reichardt, C. *Chem. Rev.* **2014**, *114*, 10429.
(16) Robert, F.; Winum, J.-Y.; Sakai, N.; Gerard, D.; Matile, S. *Org. Lett.* **2000**, *2*, 37.
(17) Martin, R. E.; Diederich, F. *Angew. Chem. Int. Ed.* **1999**, *38*, 1350.
(18) Arnaud-Neu, F.; Delgado, R.; Chaves, S. *Pure Appl. Chem.* **2003**, *75*, 71.
(19) Li, Z. H.; Wong, M. S.; Tao, Y.; D'Iorio, M. *J. Org. Chem.* **2004**, *69*, 921.
(20) Ahn, K.-H.; Ryu, G. Y.; Youn, S.-W.; Shin, D.-M. *Mater. Sci. Eng., C* **2004**, *24*, 163.
(21) Cheng, Y.-J.; Luh, T.-Y. *J. Organomet. Chem.* **2004**, *689*, 4137.
(22) Miyaura, N.; Yamada, K.; Suzuki, A. *Tetrahedron Lett.* **1979**, *20*, 3437.
(23) Barder, T. E.; Walker, S. D.; Martinelli, J. R.; Buchwald, S. L. *J. Am. Chem. Soc.* **2005**, *127*, 4685.
(24) Lennox, A. J.; Lloyd-Jones, G. C. *Chem. Soc. Rev.* **2014**, *43*, 412.
(25) Vogel, M. A.; Stark, C. B.; Lyapkalo, I. M. *Synlett* **2007**, 2907.
(26) Hoegermeier, J.; Reißig, H. U. *Chem. Eur. J.* **2007**, *13*, 2410.
(27) Rottländer, M.; Knochel, P. *J. Org. Chem.* **1998**, *63*, 203.
(28) Blettner, C. G.; König, W. A.; Stenzel, W.; Schotten, T. *J. Org. Chem.* **1999**, *64*, 3885.
(29) Dominguez, M.; Reissig, H.-U. *Synthesis* **2014**, *46*, 1100.
(30) Lou, S.; Fu, G. C. *Adv. Synth. Catal.* **2010**, *352*, 2081.
(31) Kudo, N.; Perseghini, M.; Fu, G. C. *Angew. Chem. Int. Ed.* **2006**, *45*, 1282.
(32) Lott, R. S.; Chauhan, V. S.; Stammer, C. H. *J. Chem. Soc., Chem. Commun.* **1979**, 495.
(33) Sajiki, H.; Kuno, H.; Hirota, K. *Tetrahedron Lett.* **1997**, *38*, 399.
(34) Sun, Z.; Zhou, T.; Pan, X.; Yang, Y.; Huan, Y.; Xiao, Z.; Shen, Z.; Liu, Z. *Bioorg. Med. Chem. Lett.* **2018**, *28*, 3050.
(35) Chouhan, M.; Kumar, K.; Sharma, R.; Grover, V.; Nair, V. A. *Tetrahedron Lett.* **2013**, *54*, 4540.
(36) Greene, T. W. Greene's Protective Groups in Organic Synthesis, 5th ed. John Wiley & Sons, Inc.: Hoboken, New Jersey, **2014**, 475.
(37) Bäuerle, P.; Würthner, F.; Heid, S. *Angew. Chem. Int. Ed. Engl.* **1990**, *29*, 419.
(38) Chaumeil, H.; Neuburger, M.; Jacques, P.; Tschamber, T.; Diemer, V.; Carré, C. *Tetrahedron* **2014**, *70*, 3116.
(39) (a) X-ray crystallographic data for compound **[OPP(2)-O$^-$]$_2$·HCl** were deposited in the Cambridge Crystallographic Data Centre (CCDC) with identification number 2055376. (b) X-ray crystallographic data for compound **OPP(3)-OH** were deposited in the Cambridge Crystallographic Data Centre (CCDC) with identification number 2055377.
(40) Jacques, P.; Graff, B.; Diemer, V.; Ay, E.; Chaumeil, H.; Carré, C.; Malval, J.-P. *Chem. Phys. Lett.* **2012**, *531*, 242.
(41) Effenberger, F.; Wuerthner, F.; Steybe, F. *J. Org. Chem.* **1995**, *60*, 2082.

(42) Würthner, F.; Yao, S.; Debaerdemaeker, T.; Wortmann, R. *J. Am. Chem. Soc.* **2002**, *124*, 9431.
(43) Albert, I. D. L.; Marks, T. J.; Ratner, M. A. *J. Am. Chem. Soc.* **1998**, *120*, 11174.
(44) Fabian, J.; Rosquete, G.; Montero-Cabrera, L. *J. Mol. Struct. THEOCHEM* **1999**, *469*, 163.
(45) Pati, S. K.; Marks, T. J.; Ratner, M. A. *J. Am. Chem. Soc.* **2001**, *123*, 7287.
(46) Mennucci, B. *Phys. Chem. Chem. Phys.* **2013**, *15*, 6583.
(47) Mennucci, B.; Cappelli, C.; Guido, C. A.; Cammi, R.; Tomasi, J. *J. Phys. Chem. A* **2009**, *113*, 3009.
(48) Meng, S.; Caprasecca, S.; Guido, C. A.; Jurinovich, S.; Mennucci, B. *Theor. Chem. Acc.* **2015**, *134*, 150.
(49) Frisch, M. J.; Trucks, G. W.; Schlegel, H. B.; Scuseria, G. E.; Robb, M. A.; Cheeseman, J. R.; Scalmani, G.; Barone, V.; Petersson, G. A.; Nakatsuji, H.; Li, X.; Caricato, M.; Marenich, A. V.; Bloino, J.; Janesko, B. G.; Gomperts, R.; Mennucci, B.; Hratchian, H. P.; Ortiz, J. V.; Izmaylov, A. F.; Sonnenberg, J. L.; Williams-Young, D.; Ding, F.; Lipparini, F.; Egidi, F.; Goings, J.; Peng, B.; Petrone, A.; Henderson, T.; Ranasinghe, D.; Zakrzewski, V. G.; Gao, J.; Rega, N.; Zheng, G.; Liang, W.; Hada, M.; Ehara, M.; Toyota, K.; Fukuda, R.; Hasegawa, J.; Ishida, M.; Nakajima, T.; Honda, Y.; Kitao, O.; Nakai, H.; Vreven, T.; Throssell, K.; Montgomery, J. A. Jr.; Peralta, J. E.; Ogliaro, F.; Bearpark, M. J.; Heyd, J. J.; Brothers, E. N.; Kudin, K. N.; Staroverov, V. N.; Keith, T. A.; Kobayashi, R.; Normand, J.; Raghavachari, K.; Rendell, A. P.; Burant, J. C.; Iyengar, S. S.; Tomasi, J.; Cossi, M.; Millam, J. M.; Klene, M.; Adamo, C.; Cammi, R.; Ochterski, J. W.; Martin, R. L.; Morokuma, K.; Farkas, O.; Foresman, J. B.; Fox, D. J. Gaussian 16, Revision B. 01. Gaussian Inc.: Wallingford, CT, **2016**.
(50) Lyapkalo, I.; Vogel, M.; Stark, C. *Synlett* **2007**, 2907.
(51) Pangborn, A. B.; Giardello, M. A.; Grubbs, R. H.; Rosen, R. K.; Timmers, F. J. *Organometallics* **1996**, *15*, 1518.
(52) Cowieson, N. P.; Aragao, D.; Clift, M.; Ericsson, D. J.; Gee, C.; Harrop, S. J.; Mudie, N.; Panjikar, S.; Price, J. R.; Riboldi-Tunnicliffe, A.; Williamson, R.; Caradoc-Davies, T. *J. Synchrotron Radiat.* **2015**, *22*, 187.
(53) Sheldrick, G. M. *Acta Crystallogr. Sect. C: Cryst. Struct. Commun.* **2015**, *71*, 3.
(54) Farrugia, L. J. *J. Appl. Crystallogr.* **1997**, *30*, 565.
(55) Macrae, C. F.; Bruno, I. J.; Chisholm, J. A.; Edgington, P. R.; McCabe, P.; Pidcock, E.; Rodriguez-Monge, L.; Taylor, R.; Streek, J.; Wood, P. A. *J. Appl. Crystallogr.* **2008**, *41*, 466.
(56) Brindisi, M.; Butini, S.; Franceschini, S.; Brogi, S.; Trotta, F.; Ros, S.; Cagnotto, A.; Salmona, M.; Casagni, A.; Andreassi, M.; Saponara, S.; Gorelli, B.; Weikop, P.; Mikkelsen, J. D.; Scheel-Kruger, J.; Sandager-Nielsen, K.; Novellino, E.; Campiani, G.; Gemma, S. *J. Med. Chem.* **2014**, *57*, 9578.
(57) Prodanov, M. F.; Diakov, M. Y.; Vlasenko, G. S.; Vashchenko, V. V. *Synlett* **2015**, *26*, 1905.